QA for helical tomotherapy: Report of the AAPM Task Group 148[a)]

Katja M. Langen[b)]
Department of Radiation Oncology, M. D. Anderson Cancer Center Orlando, Orlando, Florida 32806

Niko Papanikolaou
Department of Radiation Oncology, Cancer Therapy and Research Center, University of Texas Health Science Center at San Antonio, San Antonio, Texas 78229

John Balog
Mohawk Valley Medical Physics, Rome, New York 13440

Richard Crilly
Department of Radiation Medicine, Oregon Health and Science University, Portland, Oregon 97239

David Followill
Section of Outreach Physics, University of Texas M. D. Anderson Cancer Center, Houston, Texas 77030

S. Murty Goddu
Department of Radiation Oncology, Washington University School of Medicine, St. Louis, Missouri 63110

Walter Grant III
Department of Radiology/Section of Radiation Oncology, Baylor College of Medicine, Methodist Hospital, Houston, Texas 77030

Gustavo Olivera
TomoTherapy, Inc., Madison, Wisconsin 53717 and Department of Medical Physics, University of Wisconsin, Madison, Wisconsin 53706

Chester R. Ramsey
Thompson Cancer Survival Center, Knoxville, Tennessee 37916

Chengyu Shi
Department of Radiation Oncology, Cancer Therapy and Research Center, University of Texas Health Science Center at San Antonio, San Antonio, Texas 78229

(Received 9 February 2010; revised 27 April 2010; accepted for publication 15 June 2010; published 20 August 2010)

Helical tomotherapy is a relatively new modality with integrated treatment planning and delivery hardware for radiation therapy treatments. In view of the uniqueness of the hardware design of the helical tomotherapy unit and its implications in routine quality assurance, the Therapy Physics Committee of the American Association of Physicists in Medicine commissioned Task Group 148 to review this modality and make recommendations for quality assurance related methodologies. The specific objectives of this Task Group are: (a) To discuss quality assurance techniques, frequencies, and tolerances and (b) discuss dosimetric verification techniques applicable to this unit. This report summarizes the findings of the Task Group and aims to provide the practicing clinical medical physicist with the insight into the technology that is necessary to establish an independent and comprehensive quality assurance program for a helical tomotherapy unit. The emphasis of the report is to describe the rationale for the proposed QA program and to provide example tests that can be performed, drawing from the collective experience of the task group members and the published literature. It is expected that as technology continues to evolve, so will the test procedures that may be used in the future to perform comprehensive quality assurance for helical tomotherapy units. [DOI: 10.1118/1.3462971]

Key words: helical tomotherapy, quality assurance

We dedicate this task group report to the memory of Sam Jeswani. Sam was a great enthusiast of the tomotherapy technology and a tireless customer champion. Sam was the Director of Customer Relations at TomoTherapy, Inc. and a friend to many of us. Sam died during the terrorist attacks in Mumbai in November 2008.

TABLE OF CONTENTS

I. INTRODUCTION

Task Group Report 40 outlines a comprehensive quality assurance (QA) program in radiation oncology that applies to any external beam radiation therapy equipment.[1] A code of practice specific to radiotherapy accelerators is provided by Task Group Report 45.[2] Both reports are comprehensive in nature and supply fundamental guidelines to the medical physics community.

With the introduction of new technology into the field of radiation oncology, a need arises to provide guidelines that are tailored to these newer treatment modalities. The quality assurance of newer technologies is addressed in Task Group Report 142.[3] While TG-142 provides the foundation for QA guidelines of newer technologies, there are several commercially available technologies that are sufficiently different from C-arm type accelerators and require a unique set of QA recommendations. One such technology is helical tomotherapy. It is therefore the intent of this Task Group Report to provide QA guidelines for helical tomotherapy that, while based on TG-142 guidelines, are specifically adapted to this technology.

There are a fair number of the TG-142 QA recommendations that can be directly applied to helical tomotherapy (e.g., output constancy). Whenever possible, guidelines from TG-142 and other relevant task group reports have been adopted in this report. However, several traditional QA recommendations are not applicable (e.g., light field tests) to helical tomotherapy. On the other hand, important aspects of the tomotherapy treatment modality are not tested with traditional QA tests. This Task Group Report provides a comprehensive set of recommendations on all aspects of the helical tomotherapy system that should be tested and the respective recommended test frequencies. References to existing Task Group Reports are made throughout this report where appropriate. General QA guidelines such as the establishment of a departmental comprehensive QA program, as described in TG-40 are not discussed in this report.

Helical tomotherapy is an intensity modulated radiation therapy (IMRT) delivery technique that was developed at the University of Wisconsin-Madison and was later commercialized by TomoTherapy, Inc. of Madison, Wisconsin.[4] TomoTherapy, Inc. is the only vendor that markets and manufactures treatment units that use this delivery process. Procedures and recommendations discussed in this report are therefore specific to TomoTherapy's treatment units. TomoTherapy units combine IMRT treatment delivery and megavoltage computed tomography (MVCT) imaging capabilities. The units were introduced into clinical routine in 2003. Currently, more than 280 units have been installed worldwide. It is anticipated that additional Tomotherapy-specific treatment techniques will be developed in the future. Static gantry angle and dynamic y-jaw modes are currently under development. These techniques are not considered in this report. Quality assurance procedures specific to these techniques will have to be developed once those techniques become commercially available.

In this Task Group Report, an overview of the Tomo-

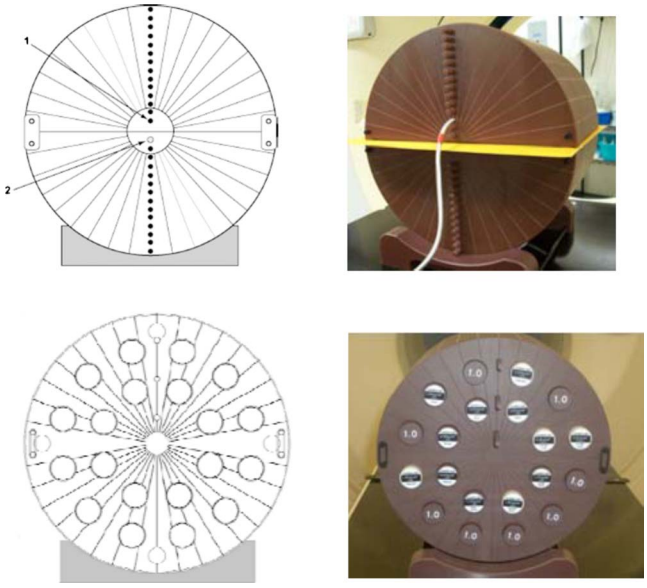

FIG. 1. Top row: Drawing and picture of a front view of the vendor supplied Virtual Water™ phantom. Each of the black circles (e.g., arrow 1) contains a Virtual Water™ plug that can be removed (arrow 2) for ion chamber insertion. The picture of the front view shows the phantom with a film inserted in the coronal plane and an ion chamber located above the film plane. Lower row: Drawing and picture of the back view of the phantom. There are 20 holes for insertion of test plugs. All holes can be filled with Virtual Water™ plugs or with a set of density calibration plugs as shown in the photo. Resolution and ion chamber plugs are also available.

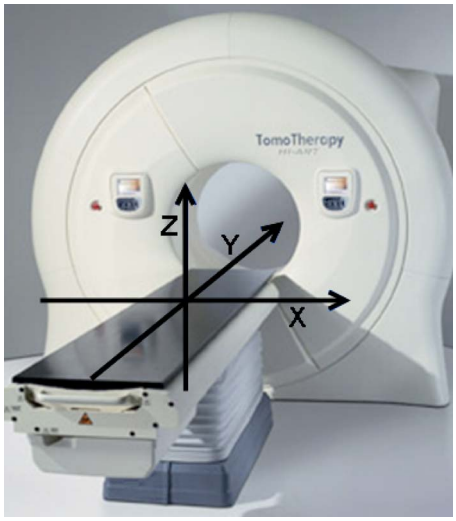

FIG. 2. The coordinate system used by TomoTherapy.

Therapy system and its unique aspects is provided. Delivery, imaging, and treatment planning quality assurance are discussed in three chapters of this report. Quality assurance aspects are summarized according to their recommended frequency in Sec. VIII. The Appendix contains a collection of useful discussions that we hope will be of interest to the practicing medical physicist.

II. GLOSSARY AND ABBREVIATIONS

Virtual Water™ phantom: A cylindrical Virtual Water™ phantom that is supplied by TomoTherapy, Inc. Tomotherapy users commonly refer to this phantom as the "cheese" phantom. This phantom can be used for various quality assurance procedures. The phantom comes apart in two hemicylinders and has holes for placing ion chambers as well as plugs for CT density tests. It has a diameter of 30 cm and a length of 18 cm. Figure 1 shows diagrams and pictures of this phantom.

TomoTherapy coordinate system convention: TomoTherapy uses the following machine coordinate system naming convention: When the patient is positioned head-first-supine on the couch, +x points toward patient's left side, +y points toward the patient's head, and +z points toward the patient's anterior side. This coordinate system is fixed, i.e., it does not rotate with the gantry. Figure 2 shows a picture of the treatment unit with the coordinate system superimposed.

DQA: Delivery quality assurance. This procedure is integrated in the TomoTherapy planning system. The patient plan is recalculated in a new CT anatomy. This new CT anatomy is typically a phantom. The DQA plan can then be delivered and the measured dose in the phantom can be compared to the calculated dose for quality assurance.

Field width/slice width: The longitudinal extent (i.e., in y-direction) of the fan beam is frequently referred to as field width in the literature. In this document, we follow the normal diagnostic radiology convention and use the term "slice width" to refer to the longitudinal extent of the treatment field.

Helical tomotherapy: The specific delivery technique.

Modulation factor: Longest leaf opening time in a plan divided by the average opening time of all nonzero leaf opening times.

MVCT: Megavoltage computed tomography.

Output: The TomoTherapy plans are based on time rather than on monitor units. The output of the machine is therefore measured in dose per unit time. Throughout this Task Group, the term output is used in this sense.

Pitch: The pitch is defined as the ratio of the couch travel per gantry rotation divided by the treatment slice width.

Sinogram: A binary file that contains data for each projection. There are several types of sinograms, such as imaging sinograms derived from detector data or control sinograms that contain fluence or MLC data for each projection or pulse.

Treatment plane: This plane marks the area that is defined by the center of the radiation field in the longitudinal (y) direction. In the x- and z-directions, this plane is parallel to the rotating fan beam.

TomoTherapy: Company that produces and markets a system that is based on a helical tomotherapy delivery technique.

Virtual isocenter: The treatment plane is located inside the bore and for convenient patient setup a virtual isocenter is defined 70 cm from the treatment isocenter in the negative y-direction. As with CT simulation, the virtual isocenter is located outside the bore and is localized via laser projections.

XML file: An XML file is generated at the end of the

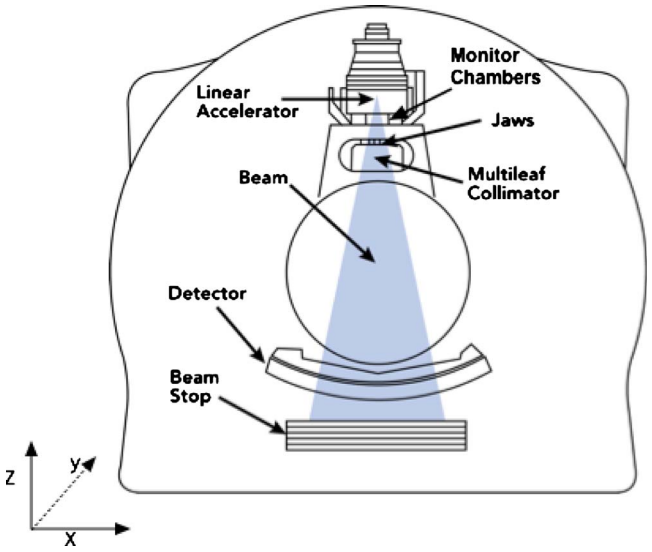

FIG. 3. Diagram of the main components of a TomoTherapy unit.

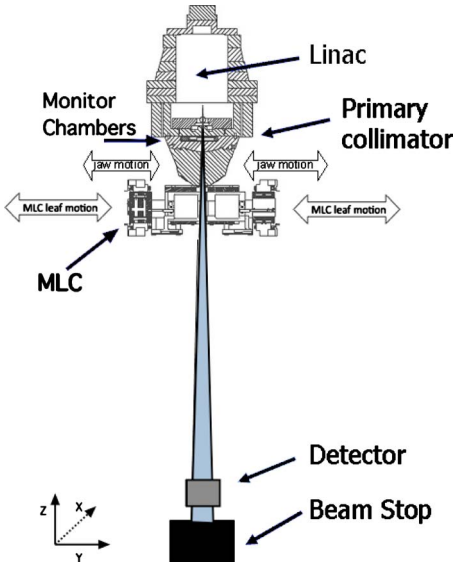

FIG. 4. Lateral view of the beam collimation components. The linac is at the 12 o'clock position in this drawing.

treatment planning process by the planning software and contains delivery instructions for the various machine components. To generate delivery instructions for QA tests, these files can also be generated independently of the treatment planning system (TPS). Tools to accomplish this are included in the operator station software.

III. SYSTEM OVERVIEW

The TomoTherapy system uses a unique geometry that resembles that of a helical CT scanner. The beam is generated by a 6 MV linear accelerator that is mounted on a slip ring gantry. The beam passes through a primary collimator and is further collimated into a fan-beam shape by an adjustable jaw. For further collimation, a binary multileaf collimator (MLC) is used. During treatment, the ring gantry continuously rotates while the patient is continuously translated through the rotating beam plane. The dose is thus delivered in a helical fashion. The ring gantry also contains a detector system that is mounted opposite the accelerator and is used to collect data for MVCT acquisition. A beam stopper is used to reduce room-shielding requirements. Figure 3 shows the general layout of the tomotherapy unit. The distance from the source to the center of rotation is 85 cm. The distance from the source to the detector is 145 cm. The Tomotherapy machine currently employs a standard detector array from a third generation CT scanner. This detector is not focused on the source but on a point that is proximal to the source. The diameter of the bore is 85 cm.

The fan beam has an extension of 40 cm in the lateral (x) direction at isocenter. In the superior-inferior, or y-direction, the beam is collimated by an adjustable jaw. In principle, this y-jaw can collimate the beam to any size that is smaller or equal to 5 cm but typically, only three distinct treatment slice widths are commissioned in the treatment planning system for clinical use. These fields have an extension of 1.0, 2.5, and 5.0 cm at isocenter in the y-direction. Figure 4 shows a diagram of the lateral view of the linac and collimation system. The TomoTherapy units do not have field flattening filters.

A binary 64 leaf collimator is used to divide the fan beam in the x-direction (with the linac at 12 o'clock). The MLC leaves travel in the y-direction as indicated in Fig. 4. Each MLC leaf is either closed or open and intensity modulation is achieved via leaf specific opening times. The MLC is pneumatically driven. It consists of two separate MLC banks. If the leaves are closed, they move across the entire treatment slice width and stop at a position beyond the treatment field under the opposite jaw. This allows a rapid transitioning (about 20 ms) of the leaf. The leaves are made from 95% tungsten and are 10 cm thick. The MLC is only focused in the lateral direction. Figure 5 shows a diagram and a photo of the MLC. The diagram also shows the MLC leaf numbering convention. All even-numbered leaves belong to the rear (located in +Y direction from isocenter) MLC bank and the odd-numbered leaves belong to the front (located in −y direction from the isocenter) MLC bank.

A beamlet is defined as the part of the treatment beam that one MLC leaf covers. The y-dimension of each beamlet at the isocenter depends on the y-jaw setting; the size of each beamlet in the x-direction is 0.625 cm (40 cm divided by 64 leaves) at the isocenter.

For the purpose of treatment planning each rotation is divided into 51 sections. These are called projections. For each projection, each MLC leaf has a unique opening time. A leaf may be open for most of the duration of the projection (with adjustments for leaf transitioning times), for part of it, or may never open during a given projection. Figure 6 illustrates the use of the MLC system during a gantry rotation for a head and neck treatment. Only every third projection is shown.

The gantry rotates clockwise if viewed from the foot of the patient couch or in the view shown in Fig. 3. The gantry

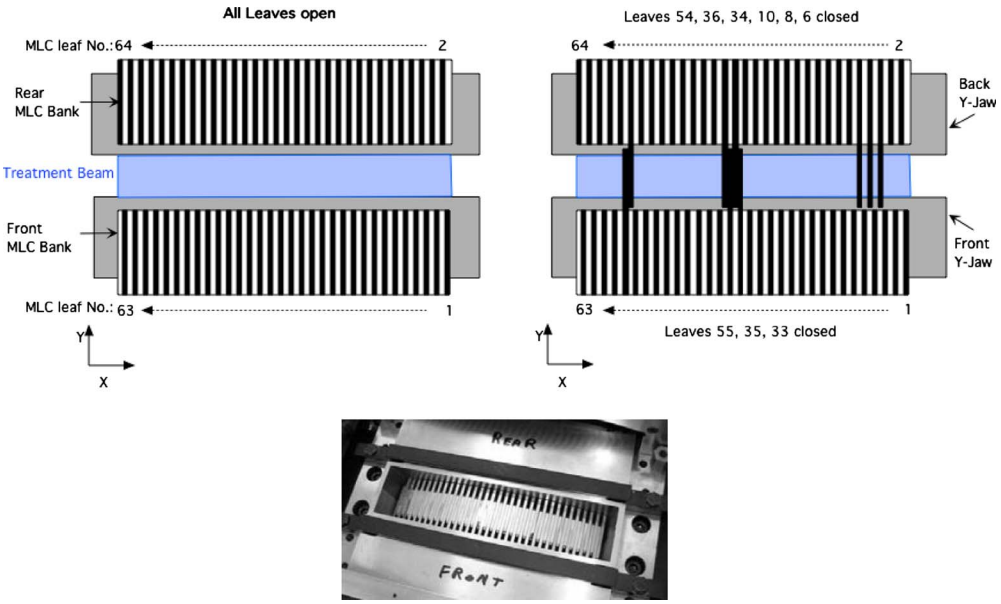

FIG. 5. A schematic drawing of the TomoTherapy MLC. The drawing on the left shows the MLC with all leaves open. The right hand drawing shows the MLC with several leaves closed. A photo of the MLC with all leaves closed is also shown. In the drawings, the MLC is in the 6 o'clock position and the observer looks down from the isocenter.

angle naming conventions conform to the International Electrotechnical Commission standard, i.e., the gantry angle is zero if the beam points downward in the vertical direction. The gantry angle increases from 0° to 359° with a clockwise rotation of the gantry.

Besides the machine hardware, two laser systems are installed in the room whose arrangement is different than what is typically found in a treatment room. The treatment plane is inside the bore and for patient setup purposes a virtual isocenter is defined outside of the bore. The distance from the virtual to the treatment plane isocenter is 70 cm in the y-direction. A fixed green laser system is used to project laser lines to the virtual isocenter. In addition, a movable red laser system is installed in the room. This laser system is similar to the laser marking systems commonly found in a CT simulator suite. The red lasers are mounted on tracks along which the laser can move. In their "home" position, the red laser lines will project to the virtual isocenter. In total, there are five red laser units in the room (two coronal, two axial, and one sagittal laser). In the treatment planning system, the red lasers can be requested to project lines to the patient setup marks. Hence, the red laser position is plan-specific. The patient may be aligned to the red or green laser system and depending on its use, the green laser system may be turned on or off during patient treatments. However, the green laser system is often used for physics tests. Figure 7 shows a diagram of the laser arrangement in the room. Only lateral and sagittal lasers are shown in this drawing. The green and red coronal laser system is not shown.

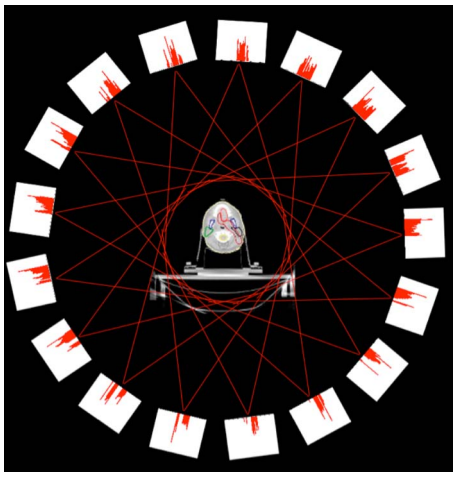

FIG. 6. Illustration of MLC use. Normalized leaf opening times are shown for every third projection of a gantry rotation during a head and neck treatment. Each of the 17 inserts shows the relative opening time (height of bar) of each of the 64 MLC leaves (represented by 64 bars along the bottom axis of each insert) during the selected projections. In these particular projections, the outer leaves are never opened since these beamlets do not pass through the tumor volume.

IV. SYSTEM SPECIFIC ACCEPTANCE AND COMMISSIONING ASPECTS

In addition to the dose delivery method and respective hardware, another unique aspect of the system is that all tomotherapy planning systems use a common beam model (several early machines had unique beam models. However, some of these early machines have subsequently been recommissioned for use with the common beam model). Each machine is adjusted in the factory such that the beam parameters match this common beam model. During the on-site acceptance testing procedure (ATP), it is verified that machine parameters still match the common beam model. Many aspects of the traditional machine commissioning tasks hence do not apply to the TomoTherapy machines. Other traditional

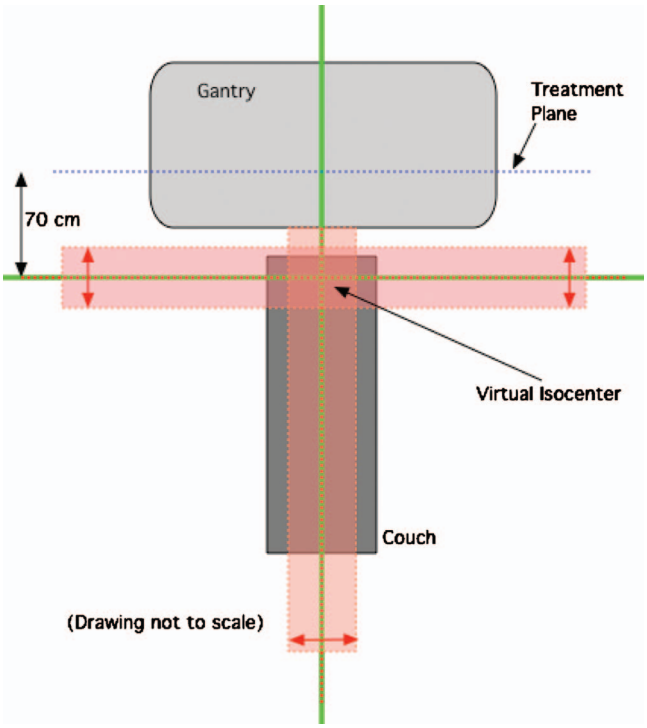

FIG. 7. A schematic drawing of the laser arrangement in the treatment room as seen from the ceiling. The green lasers are fixed and the red lasers are movable. If homed, the red laser projections overlay the green lasers. The pink box indicates the approximate area that can be occupied by the red laser system.

commissioning procedures such as the collection of baseline data for all periodic QA procedures still apply to the helical tomotherapy units.

It is recommended by this Task Group that an on-site physicist be actively involved in the acceptance testing process. He/she should collect and archive the ATP data provided by TomoTherapy, Inc. For all periodic consistency tests, the baseline data should be measured soon after machine acceptance and prior to the first treatment. All other recommended daily, monthly, quarterly, and annual QA tests should be performed once prior to the first treatment. Many of the recommended annual QA aspects are covered during the ATP process. For example, the current ATP protocol includes the mechanical alignment and beam parameter tests described in Secs. V B 1 and V B 2. Tests that are covered in the ATP process do not need to be repeated prior to the first treatment provided that the on-site physicist was actively involved in the ATP process as recommended.

V. TREATMENT DELIVERY FOR HELICAL TOMOTHERAPY

V.A. Introduction

Helical tomotherapy beam delivery is unique in its dynamics and therefore requires quality assurance tests that are tailored to this delivery technique. Some tests are similar to those performed on a conventional linear accelerator, while others are helical tomotherapy-specific.

Frequently, one aspect of the machine can be tested in different ways ranging from traditional test procedures to procedures that make use of on-board detector data acquired during helical tomotherapy procedures. Users have developed and reported tomotherapy specific test procedures.[5–7] Many of the test procedures developed by the vendor use the on-board detector while other tests are film-based. For those users that wish to use detector data, we have included in Appendix E a discussion on where the data are located and how it can be accessed. The film-based tests can be performed with radiographic or radiochromic films.

Since helical tomotherapy is still a relatively new modality, it is anticipated that test procedures will continue to evolve. The intent of this chapter is to describe what aspects of the machine should be tested. Examples of test procedures that have been developed by users or the vendor are provided. However, over time, new test procedures will likely be developed and it is not the intent of this chapter to dictate specific procedures and thus prohibit the use of better test procedures and equipment in the future.

V.A.1. Unique aspects of helical tomotherapy treatment delivery

Helical tomotherapy utilizes a dynamic delivery in which the gantry, treatment couch, and MLC leaves are all in motion during treatment. This results in highly conformal radiotherapy treatments. The complexity of the delivery is hidden from the end user due to the extensive integration and automation of the tomotherapy control systems.

There are several unique aspects of the TomoTherapy beam delivery system that the physicist needs to recognize. The machine output is defined in terms of absorbed dose per unit time rather than the traditional units of dose per monitor unit. Consequently, treatment plan parameters such as gantry rotation, table motion, and MLC openings are all time-based. A constant dose rate is assumed for treatment planning purposes and plans are terminated after the calculated time elapsed.

Two parallel-plate ion chambers are located upstream of the y-jaw and their purpose is to monitor that the dose rate is within an acceptable window. After machine calibration, the signal levels from the transmission chambers and their variation are monitored. These signal levels are referred to as the nominal rate. The establishment of the nominal rate values is performed by the vendor during ATP. Two separate monitor chamber based dose rate tests are enforced. The treatment will be terminated if (i) the monitor chamber readings differ by more than 50% from their nominal rate for more than 3 s or (ii) the monitor chamber readings differ by more than 5% from their nominal rate for more than three consecutive rolling 10 s windows. A new 10 s window is started each second such that a continuous dose rate between 50% and 95% of the nominal dose rate would trigger an interlock after 12 s. These two dose rate tests are applied to each of the two chambers independently, such that a dose rate violation detected by either chamber will interlock treatment.

The dosimetric effect that is induced by a dose rate deviation prior to treatment interruption cannot be estimated easily. Since the target volume moves through the beam plane during treatment, target volumes that have already moved out of the beam plane are not affected and neither are target volumes that have yet to move into the beam plane. Only the tissue volume that is treated during the dose rate fluctuation period is affected. The affected volume is hence defined by the fan-beam slice width plus the distance the couch moves during the dose rate fluctuation period. The fraction of the effected irradiation time depends on plan parameters. A given target voxel is scheduled to be in the beam plane for a period of time equal to the gantry rotation period divided by the pitch value. Furthermore, the dosimetric effect will depend on the MLC pattern that is executed during the dose rate fluctuation period. Hence, the dosimetric effect of dose rate fluctuations are plan-specific but are typically limited to a fraction of the irradiated volume for a fraction of its scheduled irradiation time.

The monitor chamber assembly consists of two sealed parallel-plate transmission chambers. One chamber is not segmented and the radius of the collection volume is approximately 7 cm. The signal from this volume is used to derive the monitor unit 1 signal. The second chamber is segmented into an inner volume and an outer ring volume. The inner volume has radius of approximately 5 cm. The signal from this inner volume is used to derive the monitor unit 2 signal. The outer ring is further divided into six segments. The signals from these outer segments are not used. The monitor chamber signals are accessible to the user via the auxiliary data monitoring system.

The monitor unit readings that are displayed on the operator screen are derived from the monitor chamber signals. The monitor chamber signals are scaled such that the displayed monitor units numerically agree with the machine output as expressed in cGy/min measured at a depth of 1.5 cm with an SAD of 85 cm and a 5×40 cm^2 static field. This scaling process is performed by the vendor during ATP. The displayed monitor unit rate is not the instantaneous rate but the average dose rate since the beginning of the procedure. Starting with software version 4.0, the displayed dose rate for treatment procedures is the average rate over the last 10 s, excluding the warm-up period. If 10 s have not yet elapsed since the end of warm-up, the display shows the average rate since warm-up. For QA procedures, the warm-up period is included in the displayed rate.

The output is unstable when the beam is initially turned on. This beam instability is anticipated and all MLC leaves are closed for the initial 10 s of every planned delivery. If the user generates test procedures outside of the treatment planning system, it is recommended to instruct the MLC to be closed for at least the initial 10 s of the procedure.

The procedure timing, subsystem synchronization, and procedure termination are managed via a primary timer. Three independent computer clocks are used as backup timers that will each terminate the beam 6 s after a scheduled procedure time has elapsed.

V.B. Periodic quality assurance

Throughout this section, procedures are used that require machine operation in nonstandard mode, e.g., a static gantry position may be required or noncommissioned y-jaw settings may be requested. While the user can generate these procedures on the operator station (see Appendix B), the majority of the required procedures are made available by the vendor. In this chapter, QA tests for mechanical alignment, beam parameters, synchronicity, and miscellaneous aspects are described. The calibration procedure is also contained in this chapter.

V.B.1. Mechanical alignments

Several mechanical alignments must be tested annually and whenever the alignment could be compromised. In this report, particular alignments are recommended for testing. The procedures developed by the vendor to test these alignments are acceptable test procedures. However, alternative test procedure may be developed by the user. Most tests use film dosimetry and common film or image analysis tools can be used for analysis. The vendor can also supply film analysis tools.

The first set of tests (Secs. V B 1 a, V B 1 b, and V B 1 c) check the alignment of the radiation source (i.e., the linac) against the y-jaw, MLC, and rotation plane. The second set of tests (Secs. V B 1 d, V B 1 e, and V B 1 f) check the alignment of the y-jaw and MLC with the rotation plane as well as the centering of each treatment slice.

V.B.1.a. y-jaw centering. The alignment of the radiation source in the y-direction is checked against the y-jaw. This test is performed to check that the source is centered in the collimated field. This alignment needs to be checked if any component is replaced or moved that can affect this alignment. It is recommended to check the y-jaw centering annually.

The procedure uses a 2 mm y-jaw opening that is moved in 11 steps along the y-direction. A narrow y-jaw setting amplifies the sensitivity of this test. The beam is turned on for a fixed amount of time with the y-jaw opening shifted 24, 20, 15, 10, 5, 0, −5, −10, −15, −20, and −24 mm off-axis. At each step the output is measured with a stationary long active volume ion chamber located at isocenter. The vendor uses an Exradin A17 chamber for this test. The chamber must have a linear response over a length sufficient to measure the output of the shifted beams.

The output is plotted as a function of axial jaw shift. The source is aligned with the y-jaw when beam output is at its peak, as determined by a parabolic fit to the data. An example data set from this procedure is shown in Fig. 8. The respective jaw shift may be found by using the derivative of the curve to find the apex of the parabola, which corresponds to the peak output. In the given example the derivative is, $\partial\text{signal}/\partial x=-0.0162x+0.0079$, where x is the jaw shift in mm and the peak output is at a jaw shift of 0.49 mm. The y-jaw focus point is located 5 cm above the x-ray source (i.e., 90 cm above the isocenter), which means that the source shift is magnified by a factor of 18 (i.e., 90/5) at

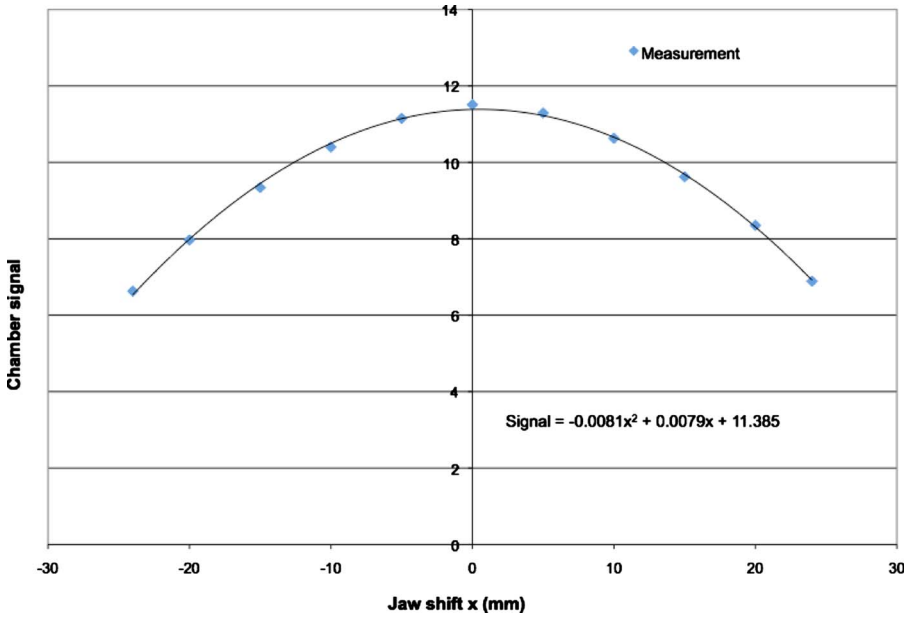

FIG. 8. An example of data measured during a y-jaw centering procedure. The measured data are fitted with a parabolic curve.

isocenter and the actual source misalignment is 0.03 mm (i.e., 0.49/18) for the given example. The vendor specification states the source position should agree with its nominal position (established at time of commissioning) within 0.3 mm. The Task Group recommends adherence to this tolerance value.

V.B.1.b. x-alignment of source. The position of the source in the x-direction is checked against the MLC position. For this test the MLC tongue and groove (T&G) effect is utilized. This effect is caused by the T&G design of the leaves that prevents a direct path for radiation to pass through when adjacent leaves are closed. A consequence of this design is a difference in the fluence output if two adjacent leaves open in sequence versus a simultaneous opening.

The T&G effect is minimized if the MLC is focused on the source. The latter fact can be used to test the source to MLC alignment. The vendor uses the MVCT detector array to collect output profiles with all even-numbered MLC leaves opened and then with all odd-numbered MLC leaves opened. This delivery sequence will maximize the T&G effect. To test the x-alignment of the source, the odd-numbered leaf profiles and even-numbered leaf profiles are added and divided by an output profile that is collected with all MLC leaves open. This normalized T&G profile should be symmetric about the center if the source is properly aligned with the MLC. Figure 9 shows normalized T&G data. An "out-of-focus" value is calculated based on the right-left asymmetry of the profile. For the purpose of calculating the out-of-focus value, the T&G profile is divided into two sides. For both sides, the average T&G signal and the standard deviation of the T&G signal is calculated. The smaller of the two average T&G signals is divided by the larger average T&G signal to calculate a ratio a that expresses the symmetry of the absolute signal. To express the symmetry of the standard deviations, two sums are calculated by separately adding each standard deviation to the overall mean T&G signal, i.e., mean signal over both sides. The smaller of the two sums is divided by the larger sum to calculate a parameter b. The vendor's out-of-focus value is based on the following formula:

$$\% \text{ out-of-focus} = 100\% \times (1 - (a + b)/2). \quad (1)$$

An empirical relationship between this value and the numerical source lateral offset has been established by the vendor. The vendor specifies a maximum out-of-focus tolerance of 2%, which corresponds to a lateral source position offset of 0.34 mm. The Task Group recommends that this test be performed in cooperation with the vendor to facilitate data collection and analysis. However, a film-based T&G procedure has been described in the literature and it can be used to independently verify the symmetry in the T&G profile.[8] The Task Group recommends adopting the vendor's tolerance for the x-alignment of the source.

V.B.1.c. y-jaw divergence/beam centering. The alignment of the y-jaw with the beam plane must be checked to assure that the central transverse axis of the treatment beam intersects the rotational axis perpendicularly, i.e., points straight down in a lateral view when the gantry is at 0° and that the beam diverges symmetrically around the plane of the gantry

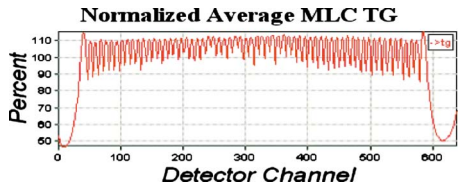

FIG. 9. The normalized tongue and groove data collected with the on-board detector array. An out-of-focus value of 1.05% was calculated from these data.

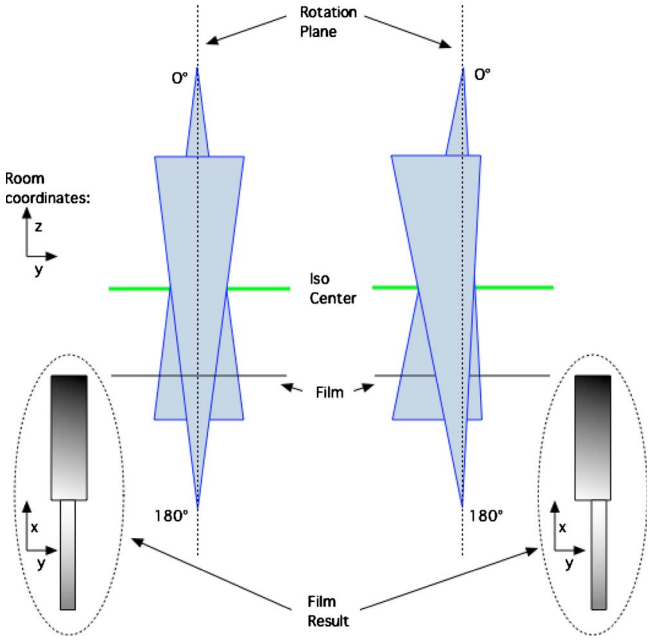

FIG. 10. Schematic of test setup for the y-divergence test. Schematic film results are shown as well. In the picture on the right hand side, the beam does not diverge symmetrically to the axis of rotation. This situation would require an adjustment of the jaw encoders.

rotation. This alignment needs to be checked if any component is replaced or moved that can affect this alignment. It is recommended to check the y-jaw/beam centering annually.

The following test procedure is acceptable to check the y-jaw divergence. A film is positioned horizontally between solid water plates (depth of 2 cm) and is positioned below the isocenter that is defined by the stationary green lasers. The film should be positioned as far as possible from the source to maximize the sensitivity of the test. Typically, the achievable distance is about 23–25 cm below isocenter. The collimation is set to define a nominal clinical field and the gantry is positioned at 0°. The MLC field is defined so that only leaves on one side of the central axis are open during exposure. The film is irradiated with the beam pointing straight down. The gantry is rotated 180° and a second irradiation is done using the same treatment slice width and MLC pattern. Figure 10 illustrates this test procedure.

A developed film of an acceptable y-divergence test is shown in Fig. 11. To test that the beam divergence is centered on the plane of gantry rotation, the center of both fields is measured. Analysis of the film involves overlaying profiles A1 and B1 of the two fields. The center of each beam is

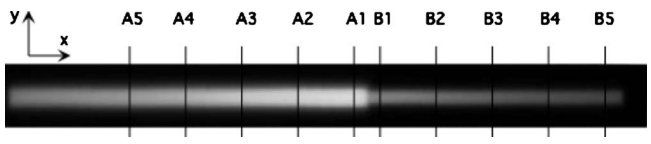

FIG. 11. Film exposure testing the alignment of the beam axial axis with the plane of rotation. For numerical analysis of the y-jaw to gantry rotation plane alignment (Sec. V B 1 d), the y-profiles are measured at several off-axis distances that cover the length of the shorter of the two beams.

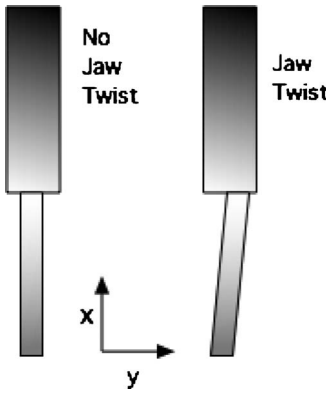

FIG. 12. Illustrations of jaw twist film results.

defined by the center of full width at half maximum (FWHM) for each beam profile (A1 and B1). A difference between the two field centers can be translated to a beam divergence at isocenter via similar triangles, i.e., divergence at isocenter=the measured difference between fields on the film multiplied by $[85\ \text{cm}/(2\times d)]$, where d is the distance from the isocenter that the film was located at. For example, with a film located 25 cm below isocenter, a 0.3 mm difference between the beam centers on the film would translate into a beam divergence at isocenter of 0.51 mm [i.e., $0.3\ \text{mm}\times(85/50)$].

The divergence of the beam axis from perpendicular at isocenter should be 0.5 mm or less per the vendor's specification. The Task Group recommends adherence to this tolerance value.

V.B.1.d. y-jaw/gantry rotation plane alignment. It should be tested that the y-jaw is parallel to the plane of rotation. This needs to be checked on an annual basis and anytime that this alignment can be compromised. The film results from the y-jaw divergence/beam centering test can be used in this analysis. Figure 12 shows sketches of acceptable and unacceptable film results.

In this instance the film profile is interrogated at several points along both fields (Positions A5–A1 and B1–B5 in Fig. 11). The y-position of the profile center is defined as the midpoint between 50% intensity penumbral position. This position is noted in both x and y for the thick and thin profiles and recorded separately. The results are plotted and the slope of the resultant straight line is ascertained. Note that the physical jaw twist equals half the angle between the fields as measured on the film. The physical jaw twist should be less than 0.5°. This is the vendor specified tolerance and the Task Group recommends adherence to this tolerance value. This tolerance ensures that the dose distribution at an off-axis distance of 10 cm has a spatial accuracy of 1 mm.

V.B.1.e. Treatment field centering. All clinical treatment fields must share a common center. This alignment should be checked if any component is replaced or moved in a way that can effect this alignment. It is recommended to check the field centering annually.

To test the field centering, a film can be placed perpendicularly to the beam axis at an 85 cm source-to-film dis-

FIG. 13. Film for test of clinical beam axial centering.

tance under a stationary vertical field. The use of solid water build-up (1–2 cm) is recommended. The control sinogram is set so that MLC leaves 11–18, 29–36, and 47–54 remain open. The y-jaws are set to the nominal width of 2.5 cm and the film is irradiated. The MLC is then set to open leaves 2–9, 20–28, 38–45, and 56–63 and movable y-jaws are set to one of the other clinical beam widths. Please refer to the MLC discussion in Sec. III for the MLC leaf numbering convention.

The film is irradiated a second time and developed. In the example shown in Fig. 13, the calibrated field of 5.0 cm is tested against the clinical 2.5 cm field. Profiles taken across the different treatment slice widths should show an agreement of the field centers within 0.5 mm at isocenter per the vendor's recommendation. The task group recommends adherence to this tolerance value. The test should be repeated for each clinical field.

V.B.1.f. MLC alignment test. The lateral alignment of the MLC relative to the center of rotation should be tested on an annual basis or after MLC replacement. Similarly, it should be tested that the MLC is aligned parallel to the rotational plane.

A film-based test can be used to test these two parameters. A film is positioned at isocenter and two central MLC leaves (32 and 33) are opened in addition to two off-center leaves (27 and 28). The film is exposed with the gantry at 0°. The gantry is moved to 180° and only the two off-center leaves are opened. The developed film should look somewhat like Fig. 14. The two outer areas should be parallel to each other (the MLC is oriented parallel to the plane of rotation). The central area should be centered between the two outer areas (no MLC lateral offset). The difference in distance between the two outer fields from the central field is used to calculate the MLC offset. It should be pointed out that any MLC offset and twist is magnified by a factor of 2 if the difference between the two outer field offsets from the central fields and the twist is measured using the above film procedure since misalignments are added from each of the two exposures. Hence, the MLC offset is equal to the difference between the right and left field offsets from the center divided by 2.

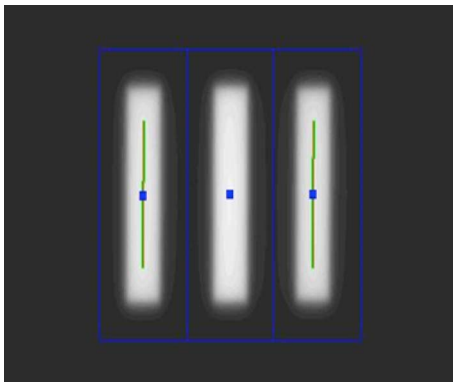

FIG. 14. MLC alignment/twist test.

Per vendor specification, the MLC offset should be less than 1.5 mm at the isocenter and the MLC twist should be less than 0.5°. The Task Group recommends that the vendor's specification be adopted.

V.B.2. Beam parameters

The unique design of the TomoTherapy treatment head results in unique beam profiles. For example, the absence of a flattening filter results in cone shaped transverse beam profiles. Monte Carlo calculations of the tomotherapy beam characteristics have been described in detail by Jeraj *et al.*[9] and Sterpin *et al.*[10]

For the purpose of routine quality assurance the consistency of the percentage depth dose, transverse, and longitudinal beam profiles, as well as the beam output should be monitored. Recommended frequencies and tolerances are discussed in the following sections. If any of these parameters vary beyond acceptable tolerance, adjustments of the machine parameters may be necessary. These adjustments require operation of the machine in service mode. Ideally, adjustments are performed by the field service engineer (FSE) and verified by the local medical physicist. At the physicist's discretion, output adjustments can also be performed and verified by the local physicist. Adjustment of the beam energy and/or beam profiles should be performed by the FSE and verified by the local physicist.

V.B.2.a. Beam quality. Agreement between the beam quality modeled in the planning systems and the measured beam quality should be tested. An example of a measured PDD is shown in Fig. 15. For comparison the modeled PDD is shown.

The standard tomotherapy PDD at a depth of 10 cm is reduced in comparison to that of a typical 6 MV linac beam due to the shorter SSD and the lower inherent energy that is due to the flattening filter free design of the tomotherapy units. However, the beam is filtered uniformly to remove low energy components.

Multiple techniques exist to measure a PDD curve and to monitor the beam energy consistency. For example, the consistency of the beam energy can be determined with a tissue maximum ratio (TMR) curve measured in a water-equivalent phantom with a simultaneous measurement of the dose rate at two depths or by measuring the beam attenuation with filters of different effective thickness.

In accordance with TG-142, the tolerance for beam quality variations is 1% for the PDD_{10} or TMR_{10}^{20}. The consistency of the beam quality should be tested on a monthly basis. This frequency is higher than the corresponding annual test recommended in TG-142. The reason for this increased test frequency is that targets wear more rapidly on TomoTherapy units than what one typically encounters in C-arm

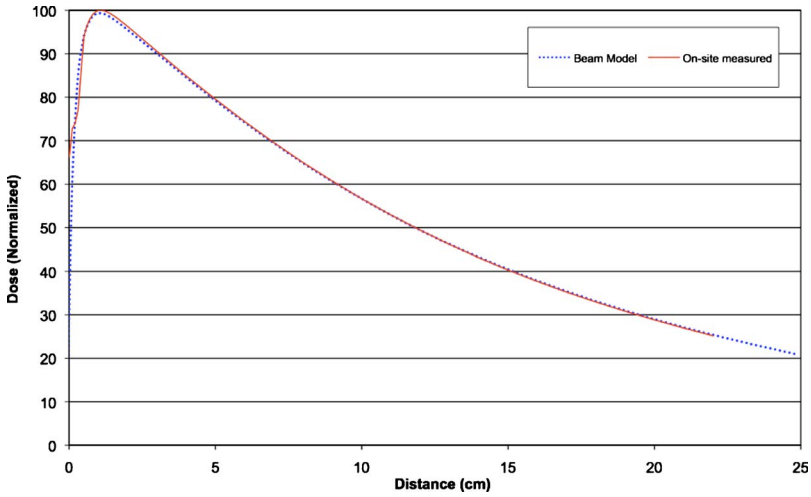

FIG. 15. Example of a PDD curve (2.5×40 cm^2 field) measured in water tank and the modeled PDD. Data were acquired at an SSD of 85 cm.

linacs. The beam quality is changing continuously throughout the lifetime of the target, but may exhibit significant dosimetric changes near the end. Accordingly, the user is advised to monitor the beam energy diligently and perhaps even further increase the frequency of beam quality monitoring if initial signs of target wear appear.[11] On an annual basis, agreement with the beam model should be verified for each commissioned treatment slice width. The beam model currently consists of PDD data in water. Hence, on an annual basis water tank data needs to be acquired for comparison with the beam data. The dimensions of water tanks are limited by the physical dimensions of the TomoTherapy bore (i.e., 85 cm). Third-party vendors have developed water tank systems that can be used in a TomoTherapy unit.

V.B.2.b. Cone (transverse) beam profiles. TomoTherapy units do not use a flattening filter and the transverse beam profiles are cone shaped. The intensity at the beam edge falls to approximately 50% of the central axis value. This is illustrated in Fig. 16. In accordance with TG-142, the consistency of the transverse beam profile size should be monitored monthly and be compared to the beam model on an annual basis. To accommodate machines without flattening filters, a beam profile consistency tolerance of 1% is specified in TG-142 for monthly beam profile tests. This value corresponds to the average absolute difference for multiple off-axis ratio measurements that are within the core of the beam (e.g., 80% of field size). The difference is specified with respect to baseline data acquired at time of commissioning. Annually, consistency of the beam profiles should be assessed against the beam model. The beam model data are available from the vendor at the time of machine installation and commissioning. Consistency can be assessed using the monthly scoring method and tolerance values.

Cone profiles can, for example, be monitored using the on-board MVCT detector system, but data access may require assistance from the TomoTherapy service engineer. Due to variations in the detector efficiency with off-axis distance, the detector data are not used to determine the beam

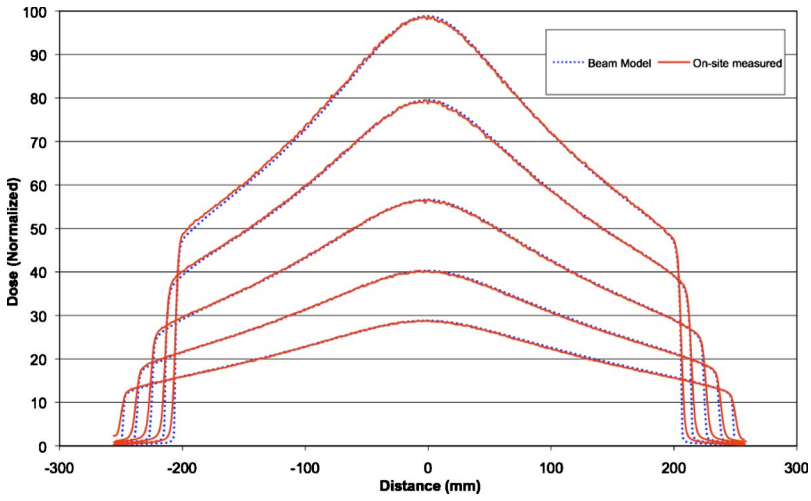

FIG. 16. Example of transverse beam profiles measured in a water tank (2.5×40 cm^2 field) and the respective modeled beam profiles. Data were acquired at an SSD of 85 cm and at depths of 15, 50, 100, 150, and 200 mm.

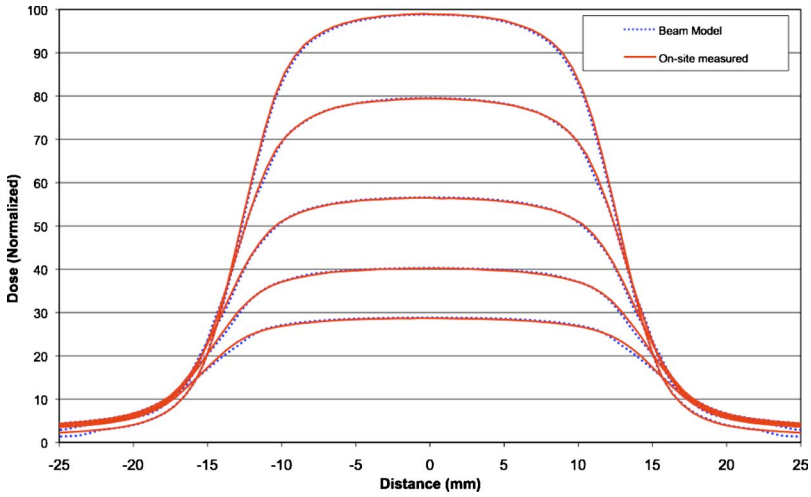

FIG. 17. Example of longitudinal beam profiles measured in a water tank and the respective modeled beam profiles. Data were acquired at an SSD of 85 cm and at depths of 15, 50, 100, 150, and 200 mm.

profile. However, changes in the beam profile result in changes of the measured detector data. Analysis of the detector data is hence a tool to test the consistency of the cone-beam profiles.[5,12] Third-party vendors have created suitable diode arrays for cone profile measurements.[12] Finally, film can be used to monitor profile consistency. Similar to possible PDD changes at the end of the target life, changes in the cone-beam profiles have been reported with target wear.[12] On a monthly basis, the transverse beam profiles should be monitored for at least one commissioned treatment slice width. On an annual basis, the agreement of the transverse beam profiles with the beam model should be tested for all commissioned treatment slice widths. Since the beam model is currently available as beam profiles in water, water tank data should be measured on an annual basis.

Inherent to the use of the on-board detector system is the assumption that the off-axis detector response remains constant over time. This assumption is not explicitly tested. The detector is rigidly attached to the gantry such that a mechanical shift is unlikely. However, if profile changes are detected with the detector system that cannot be explained by target wear or component replacements, the response of the detector system should be verified against an independent measurement such as film or diode arrays. The annual acquisition of water tank data serves as an inherent check of the detector system consistency.

V.B.2.c. Longitudinal beam profiles. The constancy of the longitudinal beam profiles is particularly important for helical tomotherapy. The dose to the patient is the integration of the longitudinal beam profile shape with couch motion (ignoring leaf modulation) and the delivered dose will therefore change if the beam profile changes.[13] For example, the delivered dose will change by approximately $\pm 10\%$ if the 1 cm beam profile changes in width by 10%, i.e., 1 mm. A careful monitoring of the beam's FWHM is hence recommended. While the constancy of the transverse beam profiles is also a test of the beam quality consistency, the longitudinal beam profile constancy test is primarily a slice width test and the beam width at half maximum is recommended for monitoring. An example of modeled and on-site measured longitudinal beam profiles is shown in Fig. 17. The consistency of the longitudinal profiles should be monitored monthly for all commissioned slice widths. Several acceptable monitoring methods exist. An electrometer can be used to sample the collected charge of an ion chamber at a frequency of several Hz, while the couch is used to move the ion chamber along the longitudinal beam profile. Note that this test procedure relies on uniform couch motion. If the profile tests fail, the uniformity of the couch motion should be evaluated (Please see Sec. V B 3 b: Couch speed uniformity). Alternatively, film dosimetry can be used to monitor the longitudinal beam profiles for consistency. The profile's FWHM should not vary by more than 1%. Hence the absolute tolerance on FWHM changes is treatment slice width specific, i.e., 0.5, 0.25, and 0.1 mm, for the 5.0, 2.5, and 1.0 cm treatment slice widths, respectively. Of the three slice widths, the 1 cm treatment slice width is the most likely to fail the 1% FWHM tolerance. Note that this test is sensitive to the setup and a failed test result should prompt setup verification. If the test result continues to fail, corrective actions (such as jaw encoder adjustments) can be performed by the vendor.

Any treatment plan that is generated in the treatment planning system requires accurate jaw settings for dosimetric accuracy. Thus, the jaw setting accuracy is inherently tested with each clinical treatment plan QA as described in Sec. VII B 3 and with the rotational output test described in Sec. V B 2 d (Output constancy). While TG-142 recommends a daily check on collimator size indicator, this Task Group recommends an explicit test of the longitudinal beam profiles on a monthly basis. More frequent testing of the longitudinal beam profiles could be prompted by failures of the treatment plan QA results.

Agreement of the measured profiles with the beam model should be verified annually. Currently water tank data should be acquired annually to enable comparison with the beam model data.

V.B.2.d. Output constancy. The consistency of the output should be monitored on a daily basis. It is recommended that the output is monitored using a stationary and/or rotational procedure. The output of the TomoTherapy unit is sensitive to the machine's operating temperature and the output should only be checked when the machine is within 2 °C of its nominal operating temperature (i.e., 40 °C). This operating temperature is monitored and regulated via a water heating and cooling circuit.

If the static output is monitored on a daily basis the rotational output should be monitored on a weekly basis and vice versa. For the stationary procedure, the gantry is stationary and a treatment field can be delivered for a specified time. Since the dose rate is initially unstable, all MLC leaves should be closed for at least the first 10 s of this procedure. A rotational procedure that mimics a patient treatment, i.e., uses a rotating gantry, moving couch, and modulated leaf opening times, should be used to test for dosimetric consistency. This procedure should be generated in the TPS.

An ion chamber or a different dosimeter with similar precision can be used for these consistency tests. The daily output checks should be consistent within a 3% window. On a monthly basis, a calibrated ion chamber should be used to measure the output using static and rotational procedures. If an ion chamber is used for the daily output check, a different chamber should be used for the monthly check. Both monthly output checks should be consistent within a 2% window. These tolerances and frequencies are in accord with those recommended in TG-142.[3]

Both output checks should be within the tolerance window. If both outputs drift in parallel, the machine output can be adjusted to rectify the situation. A more difficult situation presents itself if both outputs drift apart and only one output is within the required window. The machine service history should be reviewed to see if the beginning of the drift coincides with machine maintenance events. For example, an MLC replacement could require a replanning of the rotational procedure due to the updated leaf latency data in the TPS (please see Sec. VIII E, "Major component replacement"). The rotational output variation data should be reviewed to see if the output variations with gantry angles changed in phase or amplitude.

Tomotherapy procedures are time-based, i.e., the beam is terminated after a specified time elapses. This technique relies on constant beam output and is therefore sensitive to dose rate fluctuations. For a detailed description of the tomotherapy dose rate monitoring system, please refer to Sec. V A 1, "Unique aspects of helical tomotherapy treatment delivery." The dose rate monitoring system is based on chamber signals from two separate transmission chambers. These signals are converted to monitor unit 1 and 2 readings for display and reporting. The two raw chamber signals have separate conversion factors such that the two monitor unit rates can be numerically identical. On a monthly basis, it should be tested that the two monitor unit rate displays are consistent to within 2%. A drift between the displayed monitor units indicates a drift in the raw count rates between the two chambers. However, to re-establish that both dose rate interlocks have identical trigger levels, a reset of the nominal count rate based trigger level is required. A readjustment of two signal-to-MU conversion factors only affects the MU display but does not affect the actual trigger level. A re-establishment of the nominal count rate based trigger levels should be performed in cooperation with the vendor. The transmission chambers are only used to monitor the dose rates, i.e., they are used to interrupt a procedure if the dose rate is out of tolerance. They are not used to terminate the beam at the end of a procedure since the beam termination is time-based.

Output variations with gantry angle, i.e., rotational output variations should be monitored on a monthly basis. This test is similar to the output constancy versus gantry angle test recommended annually in TG-142. However, the rotational output on a tomotherapy unit is measured while the gantry continuously rotates. The increased test frequency that is recommended in this task group is based on the fact that the time-based output is sensitive to dose rate fluctuations with gantry angle. The rotational output variations are typically reproducible over several rotations with random variations (one standard variation) of the order of 1%–2%.[14] No information is available regarding the long-term reproducibility of the output variation with gantry rotation.

For the rotational output variation test procedure, all MLC leaves should be open and the gantry should rotate continuously. For example, rotational output measurements can be performed with an ion chamber that is placed at the isocenter or by monitoring the monitor chamber signal as a function of gantry angle.[15] The monitor chamber signal for each projection is recorded and saved as part of the patient archive (see Appendix E). To avoid beam attenuation in the treatment couch, the couch must be removed from the treatment plane, i.e., moved out of the bore, when ion chamber data are acquired.

If rotational output variation data are measured by a field service engineer as part of field service maintenance plan, the clinical physicist may review these data in lieu of a monthly measurement. The vendor's tolerance limit for the output variation with gantry angle is $\pm 2\%$ of the mean output. The tolerance for the similar TG-142 output constancy versus gantry angle test is defined relative to baseline only.[3] The Task Group recommends adherence to the vendor s tolerance value. This recommendation is based on recent findings reported in the literature.[11,14]

Since the rotational output variation is not accounted for in the treatment planning process its dosimetric effect was investigated in two recent publications. The difference in the delivered dose distribution from the planned dose distribution is smaller than the output variation since a voxel typically is irradiated from multiple gantry angles.[11,14] Flynn *et al.*[14] established a formula to calculate the acceptable amplitude of output variations as a function of the random output variations. The acceptability criterion required that the delivered dose has at least a 95% probability to be within 2% of the planned dose for all dose voxels. According to this formula the largest acceptable systematic amplitude A equals $0.34 \times (10 - \beta)$, where β is the random component of the

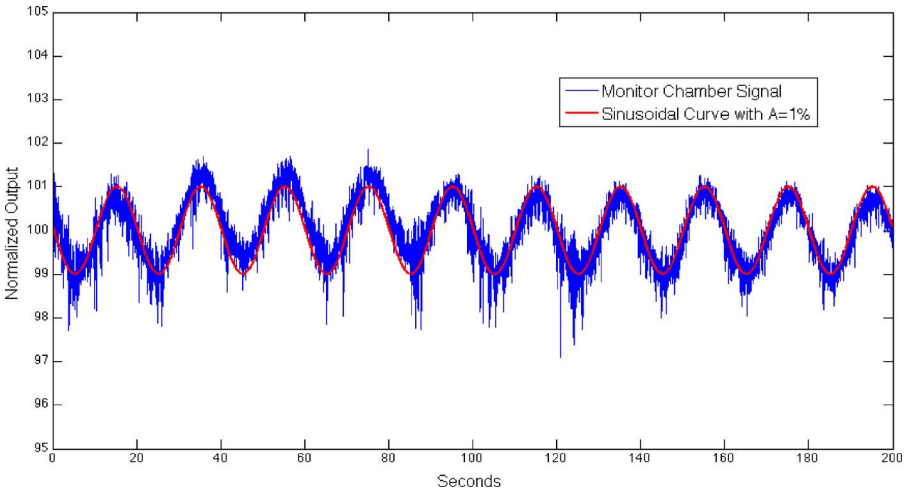

FIG. 18. Measured output variation with gantry rotation. The gantry rotation period was 20 s. A sinusoidal curve with amplitude of 1% is also shown.

output variation. Flynn *et al.*[14] consequently conclude that the vendor tolerance window of 2% is more conservative than necessary. Figure 18 shows an example of measured rotation variation data. The systematic and random (one standard variation) variation of the measured data was 1%. For this case, a systematic variation with an amplitude of 3% would have fulfilled Flynn's criteria.

V.B.3. Synchrony tests

The delivery of a helical tomotherapy plan requires synchronization between the gantry rotation and table movement. Any inaccuracy or drift in these parameters over the course of a treatment would compromise treatment accuracy. The defined tests assume standard treatment scenarios, i.e., a target with longitudinal extension up to about 20 cm. When treatments involve more complex procedures (such as TBI or CSA irradiation), these tests should be modified accordingly.

V.B.3.a. Gantry angle consistency. The ability of the system to correctly identify gantry angles should be tested periodically. It is recommended that this feature be tested quarterly. The following is an example test procedure.[6]

This test involves positioning two films parallel to the rotation plane and separated on either side of the virtual isocenter by 3 cm. A delivery sequence is defined that specifies a slice width of 2.5 cm and a pitch of 0.1 for a minimum of 40 rotations. The control sinogram is set to open the middle two leaves (32 and 33) at projections centered at 0°, 120°, and 240°. Using a horizontal line marked on the films during setup, the resulting star pattern can be checked for the correct initial angles at the start of treatment and the ability to reproduce this pattern after 24 rotations. The gantry angles should be reproducible with a tolerance of 1°.

V.B.3.b. Couch speed uniformity. The ability of the system to correctly synchronize the couch position with the beam delivery needs to be tested periodically. It is recommended to test this quarterly. The following is an example test procedure. This procedure tests for uniform couch motion.[6]

A film with 1.5 cm buildup is taped to the tabletop. An irradiation is done with a static gantry in the 0° position, the collimation set to 1 cm, all MLC leaves are opened. A couch travel distance of 20 cm for the course of the irradiation should be programmed using a couch speed that is representative of what is used clinically (e.g., 0.3–0.5 mm/s for 2.5 cm treatment slice width). The film is scanned and a profile is generated along the axis of couch travel. The relative optical density along this line should vary by less than 2%. Note that this test procedure relies on stable beam output. If this test fails, the beam output stability for static gantry procedures should be evaluated.

V.B.3.c. Couch translation/gantry rotation. The synchronization between couch translation and gantry rotation should be tested on a quarterly basis. The following describes an example test procedure.[6]

In this test, a film with 1.5 cm buildup is placed on the couch. A rotational irradiation is used with the nominal 1.0 cm beam and a pitch of 1 for 13 rotations. The control sinogram is set to open all the leaves for half a rotation on the second, seventh, and 12th rotation. The resulting film is scanned and a profile is produced along the direction of table travel. The resulting profile should show maxima 5 cm apart to within 1 mm.

V.B.4. Miscellaneous aspects

V.B.4.a. Interrupted treatment procedures. If a treatment is interrupted, the helical tomotherapy system can be used to generate a procedure to complete the treatment. The correct generation of this completion procedure should be tested monthly. This test should be performed for all commissioned slice widths on a rotating monthly schedule such that each month, one of the commissioned slice widths is scheduled for testing and each slice width will be tested every 2–3 months depending on the number of commissioned slice widths.

The following is an example test. A baseline treatment is delivered to a phantom and a coronal dose distribution is measured with film. The treatment is repeated with a new film and interrupted during the course of the treatment. A completion procedure is generated and the treatment is com-

pleted. Based on the developed films, the interrupted treatment should differ from the completed procedure by no more that 3% in its delivered dose and the overall length (FWHM) of the dose distribution in the y-direction should differ by no more than 1 mm. Since this test relies on a consistent phantom position for the interrupted and completion procedure, it is recommended to generate and deliver the completion procedure immediately after the initial treatment procedure is interrupted. It is recommended that the phantom not be moved between the deliveries of these two procedures.

V.B.4.b. Laser localization. Patients are typically positioned for treatment on the helical tomotherapy couch by aligning skin marks with wall-mounted external lasers. In theory, the use of pretreatment MVCT imaging decreases the importance of the external lasers for patient localization. In clinical practice, the use of the external lasers reduces patient rotation and aids the patient positioning process. As such, the external lasers used for helical tomotherapy units should be maintained to the same standards as used for other imaging and treatment units used in radiation oncology.

The accurate longitudinal spacing between the stationary, i.e., green, laser plane and the treatment isocenter should be tested annually using a small radiation field and a film that is marked at the virtual isocenter according to the stationary laser. The center of the radiation field should agree with the laser position to within 1 mm. The treatment field should be parallel to the laser to within 0.3° (1 mm offset at 20 cm from center). The concurrence of the virtual isocenter location and the center of the imaging plane in the x- and z-directions can be tested by imaging an object located at the intersection of the stationary lasers. This object should appear in the central MVCT pixel. Since the MVCT voxel dimensions in the "Scan"-tab are 0.8 mm in the x- and z-directions this test can test coincidence to within about ± 1 mm.

The accurate movement of the movable laser with respect to the stationary laser should be tested monthly using a predefined plan with known red to green laser offsets. The red laser movements with respect to the green laser should be within 1 mm of the planned movement.

At initialization, the green and red lasers should coincide within 1.5 mm for non-SBRT/SRS and within 1 mm for SBRT/SRS treatments. This should be tested daily. The laser systems are independent of each other and if it is found that the two systems do not coincide upon system initialization, the physicist must investigate which of the two laser systems has changed. This test inherently tests the stability of both laser systems.

V.B.4.c. Treatment couch. Tests of the treatment couch are recommended on a monthly basis. The digital readout, couch pitch, roll, and yaw, as well as the couch sag should be tested.

The agreement between physical distances traveled and the digital readout should be tested. Over a distance of 20 cm, the agreement should be within 1 mm. Since the vertical couch position causes a longitudinal shift of the couch, the proper longitudinal position in the room coordinate system should be checked at different couch heights.

The leveling of the stationary couch should be tested and the pitch and roll should be less than 0.5°. The longitudinal couch movement should be perpendicular to the treatment plane. This can be tested by checking the couch alignment against the sagittal laser at different longitudinal couch positions. Over the distance of 20 cm, the lateral couch position should deviate by less than 1 mm. At the isocenter, the couch sag between the virtual isocenter and the treatment plane should be less than 5 mm for an unloaded couch per the vendor's specifications.

V.B.5. Calibration

V.B.5.a. TG-51 equivalent calibration of the static beam. The development and clinical use of helical tomotherapy units has presented a challenge to the medical physics community. Helical tomotherapy units require a calibration of their dose output in the same manner and with the same accuracy as performed for conventional C-arm-gantry-based therapeutic accelerators. The recommended protocol for clinical reference dosimetry of high-energy photons in North America is the American Association of Physicists in Medicine TG-51 report.[16] This protocol is based on an ionization chamber having a ^{60}Co absorbed-dose to water calibration factor from an Accredited Dosimetry Calibration Laboratory (ADCL), the National Institute of Standards and Technology (NIST) or the National Research Council (NRC) in Canada. The formalism used by the TG-51 protocol is the following:

$$D_w^Q = M \cdot k_Q \cdot N_{D,w}^{^{60}\mathrm{Co}}, \tag{2}$$

where D_w^Q is the absorbed-dose to water at the point of measurement of the ionization chamber when it is absent, M is the fully corrected electrometer reading, $N_{D,w}^{^{60}\mathrm{Co}}$ is the ^{60}Co absorbed-dose to water calibration coefficient, and k_Q is the beam quality conversion factor, which accounts for the change in the absorbed-dose to water calibration coefficient between the beam quality of interest Q and the ^{60}Co beam quality for which the absorbed-dose calibration factor was determined by the ADCL. The k_Q values to be used with the TG-51 protocol have been tabulated in TG-51 as a function of the percent depth dose specified at 10 cm and 100 cm SSD for a 10×10 cm^2 reference field size in the clean, electron contamination-free photon beam. For several commercially available radiation therapy devices, it is not possible to measure the percent depth dose under these reference conditions. In recognition of this problem, the AAPM has formed a "Working Group on Dosimetry Calibration Protocols for Beams that are not Compliant with TG-51" to develop appropriate calibration procedures in collaboration with the International Atomic Energy Agency (IAEA).

The helical tomotherapy physical limitations do not permit a 10×10 cm^2 field size at 100 cm SSD. However, a 5 cm$\times$10 cm field size can be set at 85 cm SSD. In the longitudinal (y) direction, the maximum field dimension is 5 cm. Furthermore, there is a maximum distance of only 28 cm from isocenter to the lowest extend of couch position. This does not allow for an accurate measurement of the photon component percent depth dose at a 10 cm depth at 100 cm

SSD since there would not be sufficient phantom material for appropriate backscatter. In addition, since the helical tomotherapy unit does not have a flattening filter, depth dose data are slightly different than the depth dose data for similar nominal photon energies that have passed through a flattening filter. Since the TG-51 geometrical PDD reference conditions cannot be achieved, an alternate method of determining the helical tomotherapy beam quality is needed that will allow the use of the TG-51 tabulated k_Q values when performing a reference calibration of the helical tomotherapy unit.

The IAEA-AAPM joint committee proposed a formalism to determine the absorbed-dose to water to a static beam under specific helical tomotherapy reference conditions.[17] This field is called a *machine-specific reference* (msr) field. The msr field is a static field that uses reference conditions that are achievable on a helical tomotherapy machine (i.e., a 5×10 cm^2 field size at an SSD of 85 cm).

The Task Group recommends that this proposed formalism be followed until a formal protocol is established. The following equation, which is an extension of the TG-51 calibration protocol, details the proposed calculation of the absorbed-dose to water (the proposed formalism uses the IAEA TRS-398 nomenclature.[18] This nomenclature is adapted hence forth to facilitate comparison with the original publication of Alfonso *et al.*[17]):

$$D_{w,Q_{\mathrm{msr}}}^{f_{\mathrm{msr}}} = M_{Q_{\mathrm{msr}}}^{f_{\mathrm{msr}}} \cdot N_{D,w,Q_0} \cdot k_{Q,Q_0} \cdot k_{Q_{\mathrm{msr},Q}}^{f_{\mathrm{msr}},f_{\mathrm{ref}}}, \tag{3}$$

where Q is the beam quality $[\%dd(10)_x]$ of the conventional reference field 10×10 cm^2 at 100 cm SSD according to TG-51 protocol; Q_{msr} is the beam quality $[\%dd(10)_x]$ of the machine-specific reference field f_{msr} (5 cm$\times10$ cm field at 85 cm SSD); $M_{Q_{\mathrm{msr}}}^{f_{\mathrm{msr}}}$ is the corrected reading of the dosimeter for the field f_{msr}; N_{D,w,Q_0} is the absorbed-dose to water calibration factor for a reference beam quality Q_0 (usually ^{60}Co) determined by the standards laboratory (ADCL or NRC); k_{Q,Q_0} is the beam quality correction factor for beam quality Q of the conventional reference field f_{ref} (10×10 cm^2 at 100 cm SSD); and $k_{Q_{\mathrm{msr},Q}}^{f_{\mathrm{msr}},f_{\mathrm{ref}}}$ is the factor to correct for the differences between the conditions of field size, geometry, phantom material, and beam quality of the conventional reference field f_{ref} and the machine-specific reference field f_{msr}.

A key product in the equation presented above is $k_{Q,Q_0}\times k_{Q_{\mathrm{msr},Q}}^{f_{\mathrm{msr}},f_{\mathrm{ref}}}$, which converts the calibration factor from calibration beam to the machine-specific reference beam, i.e.,

$$K_{Q,Q_0}\times k_{Q_{\mathrm{msr},Q}}^{f_{\mathrm{msr}},f_{\mathrm{ref}}} = \frac{[(L/\rho)_{\mathrm{air}}^{\mathrm{water}} P_{\mathrm{wall}} P_{\mathrm{repl}} P_{\mathrm{cel}}]_{\mathrm{HT(SSD=85\ cm,}FS=5\times10\ \mathrm{cm^2,depth=10\ cm)}}}{[(L/\rho)_{\mathrm{air}}^{\mathrm{water}} P_{\mathrm{wall}} P_{\mathrm{repl}} P_{\mathrm{cel}}]_{^{60}\mathrm{Co(SSD=100\ cm,FS=10\times10\ cm^2,depth=10\ cm)}}}, \tag{4}$$

where $(L/\rho)_{\mathrm{air}}^{\mathrm{water}}$ is the ratio of the mean restricted mass collision stopping power; P_{wall} is the ionization chamber wall correction factor; P_{repl} is the fluence and gradient correction factor; and P_{cel} is a correction factor for the presence of a central electrode.

A method to determine this correction factor is described by Thomas *et al.*[19] In their publication, the correction factor is called $k_{Q(\mathrm{HT\ TG\text{-}51})}$, where HT stands for helical tomotherapy. Since the calibration correction factor k_Q is specified in TG-51 as a function of the percentage depth dose at 10 cm depth in a 10×10 cm^2 field size at 100 cm SSD, i.e., $\%dd(10)_{x[\mathrm{HT\ TG\text{-}51}]}$, Thomas derived a conversion function for this specifier to the beam quality $\%dd(10)_{x[\mathrm{HT\ ref}]}$ measured in the tomotherapy reference field (10 cm depth, 85 cm SSD, 5×10 cm^2 field size). The relationship was plotted and a third order polynomial [Eq. (5)] was fitted to the data as seen in Fig. 19.

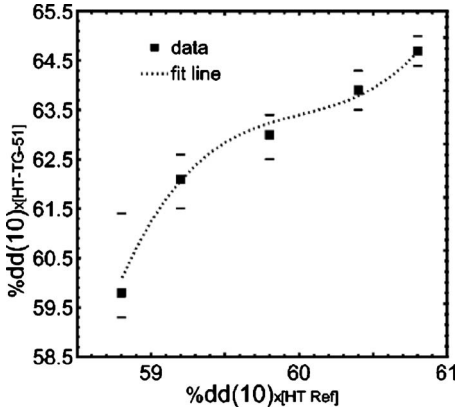

FIG. 19. The relationship between $\%dd(10)_{x[\mathrm{HT\ ref}]}$ and $\%dd(10)_{x[\mathrm{HT\ TG\text{-}51}]}$. [Reproduced from Thomas *et al.* (Ref. 19)].

The polynomial as derived by Thomas *et al.* is expressed in Eq. (5),

$$\begin{aligned}\%dd(10)_{x[\mathrm{HT\ TG\text{-}51}]} = {} & 1.35805\cdot(\%dd_{(10)x[HT\ ref]})^3 \\ & - 244.493\cdot(\%dd_{(10)x[\mathrm{HT\ ref}]})^2 \\ & + 14672.98\cdot\%dd_{(10)x[\mathrm{HT\ ref}]} \\ & - 293479.4.\end{aligned} \tag{5}$$

The maximum error in the fit of Eq. (5) is 0.3%. In order to use this relationship shown in Eq. (5), one must measure $\%dd(10)_{x[\mathrm{HT\ ref}]}$ with an ionization chamber of the appropriate size. Since the helical tomotherapy photon beam is unflattened, the beam profile in the cross-plane direction is peaked and there exists only a small portion of the profile (<2 cm) where the beam may be considered uniform and

TABLE I. Values of k_Q for photon beams as a function of the beam quality $\%dd(10)_x$ for cylindrical ionization chambers commonly used for clinical reference dosimetry. The tabulated values can be interpolated linearly in $\%dd(10)_x$. The ionization chamber specifications are found in Table III of the TG-51 protocol. Values for the A1SL chamber are from Thomas *et al.* (Ref. 19).

	k_Q		
	Beam quality specifier $\%dd(10)_x$		
Ion chamber	58	63	66
Capintec PR-05/PR-05P	0.999	0.997	0.995
ExradinAl Shonka[a]	0.999	0.998	0.996
ExradinA12 Farmer	1	0.999	0.996
Exradin A1SL miniature Shonka	0.999	0.998	0.996
PTWN30001 0.6cc Farmer[b]	1	0.996	0.992
PTW N30002 0.6cc all Graphite	1	0.997	0.994
PTW N30004 0.6cc Graphite	1	0.998	0.995
PTW 31003 0.3cc waterproof[c]	1	0.996	0.992
WellhoferIC-10/IC-5	1	0.99	0.996

[a]The cavity radius of the A1 here is 2 mm although in the past Exradin has designated chambers with another radius as A1.
[b]PTW N30001 is equivalent to the PTW N23333 it replaced.
[c]PTW N31003 is equivalent to the PTW N233641 it replaced.

flat. The $\%dd(10)_{x[\text{HT ref}]}$ should only be measured with ionization chambers whose transverse diameter is smaller than the flat portion of the curve. This size requirement will ensure that the percent depth dose measurements are made in the flat portion of the beam minimizing volume averaging and reducing any error associated with centering the chamber in the beam. Conventional farmer chambers, such as those listed in Table I, whose diameter do not exceed 6.3 mm are small enough to fulfill this requirement.

The relationship shown in Fig. 19 was derived based on using an Exradin A1SL ionization chamber (Standard Imaging, Middleton, WI), but is applicable to other ionization chambers as long as the ionization chamber size limitations are met and correct percent depth dose data are measured incorporating the correct shift ($0.6r_{cav}$) to the effective point of measurement as defined by TG-51.

Another consideration in determining the helical tomotherapy unit beam quality is that any small error in the resulting $\%dd(10)_{x[\text{HT ref}]}$ will not significantly affect the k_Q value used in the calculation of the reference absorbed dose. For the range of $\%dd(10)_{x[\text{HT ref}]}$ values, i.e., 60%–64%, associated with the measured $\%dd(10)_{x[\text{HT ref}]}$ values on a helical tomotherapy unit, the k_Q values are nearly constant for the most commonly used cylindrical ionization chambers found in TG-51 and Thomas *et al.*, varying from 0.999 to 0.995, respectively.[16,19] Any small error in the determination of $\%dd(10)_{x[\text{HT TG-51}]}$ will result in an error of typically no more than 0.1% in the final calculation of the reference absorbed dose.

The method recommended by this Task Group to determine the helical tomotherapy beam quality and the resulting $k_{Q,Q_0} \times k_{Q_{\text{msr}},Q}^{f_{\text{msr}},f_{\text{ref}}}$ product is to use the equivalent beam quality specifier technique described by Thomas *et al.*[19] described above. This particular method requires the physicist to determine the beam quality specifier $\%dd(10)_{x[\text{HT ref}]}$, i.e., the percent depth dose in water at 10 cm depth at 85 cm SSD for a 5×10 cm^2 field size and use the relationship defined by Thomas *et al.* to determine the equivalent beam quality specifier $\%dd(10)_{x[\text{HT TG-51}]}$. Once the equivalent beam specifier $\%dd(10)_{x[\text{HT TG-51}]}$ is known, the k_Q values listed in Table I and TG-51 are used to substitute the $k_{Q,Q_0} \times k_{Q_{\text{msr}},Q}^{f_{\text{msr}},f_{\text{ref}}}$ product in Eq. (3). It should be noted that Table I is a reproduction of Table I from TG-51 and includes the k_Q values for the Exradin A1SL ionization chamber calculated by Thomas *et al.*[19,20]

The calibration protocol for the helical tomotherapy unit is then similar to the procedures stated in the TG-51 protocol.

(1) Position the ionization chamber in a water phantom such that the center electrode is at a depth of 10 cm at 85 cm SSD or SAD for a 5×10 cm^2 field size. Allow the ionization chamber to equilibrate to the temperature of the phantom which should be at room temperature.
(2) Record the temperature and pressure readings to determine the temperature/pressure correction, P_{TP}.
(3) Take ionization readings per unit time at full bias to obtain M_{raw} readings.
(4) Take ionization readings per unit time at half bias to obtain your M_{raw}^{L} readings to determine the ion recombination factor P_{ion} per TG-51.
(5) Take ionization readings per unit time at the opposite polarity of the full bias reading to obtain your M_{raw}^{+} readings to determine the polarity correction P_{pol} per TG-51.
(6) Calculate the corrected ionization chamber reading per TG-51:

$$M_{Q_{\text{msr}}}^{f_{\text{msr}}} = M_{\text{raw}} \cdot P_{\text{TP}} \cdot P_{\text{ion}} \cdot P_{\text{pol}} \cdot P_{\text{elec}}. \quad (6)$$

(7) Calculate the dose to water per unit time at a depth of 10 cm using

$$D_{w,Q_{\text{msr}}}^{f_{\text{msr}}} = M_{Q_{\text{msr}}}^{f_{\text{msr}}} \cdot N_{D,w,Q_0} \cdot k_{Q,Q_0} \cdot k_{Q_{\text{msr}},Q}^{f_{\text{msr}},f_{\text{ref}}}. \quad (7)$$

(8) Calculate the dose to water per unit time at $d_{\max}$ using the clinical $\%dd(10)$ for SSD setup or the clinical TMR(10) for SAD setup.

One can be assisted by the worksheet in Appendix A for calculation of the static output of the helical tomotherapy machine. The worksheet is based on worksheet A of the TG-51 protocol.[16]

Although the static output calibration is done in a delivery mode that is not used for the treatment of patients, it forms a valuable part of the machine QA. This mode excludes all treatment dynamics and allows the determination of a single but fundamental machine characteristic. In addition, the static output calibration satisfies most state regulations that require the physicist to calibrate their machine once a year using an established calibration protocol. The methodology

described above is a simple extension of the TG-51 protocol and as such should satisfy the annual calibration requirement within the state regulations.

V.B.5.b. Output calibration (rotational procedure). Since patients are not treated with a stationary unmodulated beam, but rather with a rotating beam the output of the helical tomotherapy unit should be verified under these conditions. The IAEA/AAPM formalism mentioned earlier has addressed this issue for helical tomotherapy machines.[17] In addition to static-field dosimetry it allows a second calibration route that is based on the delivery of composite fields. The formalism suggests that the physicist will develop a *plan-class specific reference* (pcsr) field and perform the measurements within this field to determine the output of the machine as it rotates about the calibration phantom. This pcsr field according to the IAEA/AAPM formalism "is as close as possible to a final clinical delivery scheme, but delivers a homogeneous absorbed dose to an extended and geometrically simple target volume."

The pcsr field should be designed to provide a uniform dose over a region exceeding the dimensions of the reference detector. While the IAEA/AAPM formalism does not specify the particulars of the pcsr field, the recommendation of this task group is to generate a treatment plan that delivers a uniform dose of 2 Gy to a target of 8 cm diameter and 10 cm length in a 30 cm diameter water-equivalent phantom that has a minimum length of 15 cm. The vendor supplied Virtual Water™ phantom fulfills these requirements. It is recommended to use a 5 cm treatment slice width and a pitch of 0.287. For a detailed discussion of the treatment planning parameters and a discussion of phantom-based treatment plans the reader is referred to Sec. VII. The cylindrical water-equivalent phantom is imaged using a CT scanner and a treatment plan to deliver a homogeneous dose to the pcsr field is developed. The phantom should be scanned without the ionization chamber present. After the plan has been calculated, the volume that will be occupied by the active chamber volume is identified in the CT image and the average calculated dose to this volume is used for comparison with the measurements.

The phantom is placed on the treatment couch with the appropriate ionization chamber located in the center of the pcsr field. Ionization measurements (accumulating charge for the time interval to deliver the plan) are collected while delivering the plan with the homogeneous dose distribution.

The absorbed dose in a pcsr field can be calculated using the following equation, which is an extension of Eq. (3).

$$D^{f_{\mathrm{pscr}}}_{w,Q_{\mathrm{pscr}}} = M^{f_{\mathrm{pcsr}}}_{Q_{\mathrm{pcsr}}} \cdot N_{D,w,Q_o} \cdot k_{Q,Q_o} \cdot k^{f_{\mathrm{msr}},f_{\mathrm{ref}}}_{Q_{\mathrm{msr}},Q} \cdot k^{f_{\mathrm{pcsr}},f_{\mathrm{msr}}}_{Q_{\mathrm{pcsr}},Q_{\mathrm{msr}}}, \qquad (8)$$

where $M^{f_{\mathrm{pcsr}}}_{Q_{\mathrm{msr}}}$ is the corrected reading of the dosimeter in the field f_{pcsr}; $k^{f_{\mathrm{pcsr}},f_{\mathrm{msr}}}_{Q_{\mathrm{pcsr}},Q_{\mathrm{msr}}}$ is the factor to correct for the differences between the conditions of field size, geometry, phantom material, and beam quality of the machine-specific reference field f_{msr} and the plan-class specific reference field f_{pcsr}. $k^{f_{\mathrm{pcsr}},f_{\mathrm{msr}}}_{Q_{\mathrm{pcsr}},Q_{\mathrm{msr}}}$ is equal to 1.003 for most commonly used ionization chambers. (In the IAEA/AAPM formalism, a $k^{f_{\mathrm{msr}},f_{\mathrm{ref}}}_{Q_{\mathrm{msr}},Q}$ value of 0.997 is listed for helical tomotherapy msr field sizes of 5×10 cm^2. For helical tomotherapy, pcsr field deliveries with 5, 2.5, and 1 cm field $k^{f_{\mathrm{pcsr}},f_{\mathrm{ref}}}_{Q_{\mathrm{pcsr}},Q}$ values of 1.000, 1.000, and 0.997 are listed for a NE2611 chamber.[17] This allows the calculation of a $k^{f_{\mathrm{pcsr}},f_{\mathrm{msr}}}_{Q_{\mathrm{pcsr}},Q_{\mathrm{msr}}}$ value of 1.003 for 5 cm and 2.5 cm pcsr field deliveries. However, the reported $k^{f_{\mathrm{pcsr}},f_{\mathrm{ref}}}_{Q_{\mathrm{pcsr}},Q}$ factors have a significant standard uncertainty of 0.8%.[17] Revised $k^{f_{\mathrm{pcsr}},f_{\mathrm{ref}}}_{Q_{\mathrm{pcsr}},Q}$ factors may be published in the future and appropriate adjustment to the $k^{f_{\mathrm{pcsr}},f_{\mathrm{msr}}}_{Q_{\mathrm{pcsr}},Q_{\mathrm{msr}}}$ factor may be required at that time.)

The physicist should follow the same procedure as outlined for the static beam output calibration to determine the beam quality for the machine-specific reference field, $\%dd(10)_{x[\mathrm{HT\ TG\text{-}51}]}$ and using Thomas *et al.*'s relationship determine the beam quality of the conventional reference field $\%dd(10)_{x[\mathrm{HT\ ref}]}$. Knowing the beam quality, one can determine the $k_{Q,Q_0}\times k^{f_{\mathrm{msr}},f_{\mathrm{ref}}}_{Q_{\mathrm{msr}},Q}$ product for the specific chamber used in the calibration. The corrected meter reading for the pcsr field $M^{f_{\mathrm{pcsr}}}_{Q_{\mathrm{pcsr}}}$ should be determined as outlined in the worksheet in Appendix A. The worksheet in Appendix A can be used to assist in the calculation of the absorbed dose to the plan-class specific reference field $D^{f_{\mathrm{pcsr}}}_{w,Q_{\mathrm{pcsr}}}$ per Eq. (8). The absorbed-dose to water for the pcsr field is delivered in the same mode that is used to deliver patient treatments. The absorbed dose determined under the pcsr conditions can be compared to the value calculated by the tomotherapy planning software. If differences between the calculated and measured dose are identified that are in excess of 1%, it is recommended by this task group to make adjustments to the machine output.

The static calibration procedure described in Sec. V B 5 a should form part of the calibration procedure, but its use is limited since the expected output under static conditions cannot be compared to an expected value from the planning system. The calibration of the tomotherapy unit via pcsr fields is hence the relevant calibration route.[17]

V.B.5.c. Independent verification of calibration. It is recommended that an independent verification of the tomotherapy calibration be performed prior to the initial patient treatment and that it is repeated on an annual basis. The Radiological Physics Center in Houston (rpc.mdanderson.org/RPC/home.htm) offers a mail-in TLD monitoring service that can be used for an independent verification by NCI clinical trials participants. Other facilities are advised to contact one of the for-fee remote auditing services such as Radiation Dosimetry Services (www.mdanderson.org/education-and-research/resources-for-professionals/scientific-resources/core-facilities-and-services/radiation-dosimetry-services/index.html). Local regulation may also require an independent verification of machine calibration.

VI. TREATMENT IMAGING FOR HELICAL TOMOTHERAPY

VI.A. Introduction

In addition to its ability to deliver IMRT, the TomoTherapy system also has the ability to obtain images of the

patient in the treatment position prior to each treatment. These images are acquired to check and correct, if necessary, the patient's position for treatment. Inaccurate patient positioning will result in a geographic misplacement of the dose distribution.

The AAPM TG-142 report includes recommendations on serial and cone-beam CT for image guidance.[3] Periodic tests of geometric accuracy, image quality, and imaging dose are recommended in TG-142. The intent of Sec. VI A 1 is to describe respective quality assurance procedures associated with the imaging aspect of the TomoTherapy unit.

VI.A.1. Unique aspects of megavoltage CT imaging

The radiation beam that is used for imaging on the TomoTherapy unit is generated by the same linear accelerator that is used to generate the treatment beam. Therefore, the beam energy is in the megavoltage range and the image modality is referred to as MVCT imaging. For MVCT imaging, the accelerator is adjusted such that the nominal energy of the incident electron beam is 3.5 MeV.[9] The detector used in the TomoTherapy system is an arc-shaped CT xenon detector that has been described previously.[21–23] The standard image matrix size is 512×512 pixels and the field-of-view has a diameter of 40 cm. A filtered back-projection algorithm is used for image reconstruction.[23]

On the user interface, the operator is tasked with the selection of the scan length and the slice thickness. Three pitch values (1, 2, and 3), are pre-programmed; these are referred to as fine, normal, and coarse, respectively. The standard y-jaw setting for the imaging mode is 4 mm and the pre-programmed pitch values correspond to a nominal slice thickness of 2, 4, and 6 mm. The rotational period during the image acquisition is fixed at 10 s. Using a half-scan reconstruction technique, this translates to an acquisition rate of 1 slice per 5 s. The imaging dose depends on the selected pitch and the thickness of the imaged anatomy, but it is typically in the range of 1–3 cGy.[24] The total scan time depends on the number of selected slices.

The TomoTherapy operator station includes image registration tools for manual or automatic rigid-body registration. The automatic registration tools are typically faster than manual image registration, but it is important that automatically registered images are checked for accuracy by an experienced user.

The dimensions of the kVCT and MVCT image voxels are different in size. The kVCT image, which has a variable field-of-view, is typically down-sampled to a 256×256 matrix upon import to the TPS while the MVCT image has a 512×512 matrix size with a 40 cm field-of-view. During automatic image registration, a nearest neighbor approach is used for image interpolation.

A registration accuracy on the order of one-half voxel dimension can be expected for phantom MVCT to kVCT image registrations under these ideal conditions.[25,26] The larger of the two voxel dimensions, kVCT or MVCT, is the limiting one. In the y-direction, the MVCT voxel size varies with the imaging pitch, and the superior-inferior registration precision reduces with an increase in the MVCT slice thickness.[26]

VI.B. Periodic quality assurance

VI.B.1. Spatial/geometry tests

The primary purpose of MVCT imaging is image guidance. Accordingly, the geometric accuracy of the reconstructed images and the accuracy and consistency of the image registration procedure should be tested. Appropriate phantom-based test procedures are described below.

It should be pointed out that the image registration precision will depend on the available image content, i.e., it could depend on the test phantom itself. For example, a high contrast object that is easy to identify in both images (e.g., a metal ball of 1–2 mm diameter) can be registered more precisely than a phantom that varies little in the superior-inferior direction. Similarly, the scan range and parameters influence the available information and this can affect the registration precision.[26,27] It should further be understood that registering patient images can be more subjective depending on the anatomical site because anatomical changes in the patient can add a level of complexity and subjectivity that is absent from rigid phantom alignments. The clinical registration precision can be determined using actual patient images, clinical operators, and clinical alignment techniques.[28]

VI.B.1.a. Geometric distortions. The accurate reconstruction of an object in the MVCT image in terms of dimension and orientation can be tested with a rigid phantom of known dimensions and orientation. The recommended test frequency is monthly. The vendor supplied cylindrical Virtual Water™ phantom or a phantom of similar size can be used.

Distances between embedded objects in the x-, y-, and z-directions, and the orientation of the phantom as they appear in the MVCT image can be compared to the physical distances and orientation of the phantom. The use of small fiducial markers that are embedded or attached to the phantom will increase the precision of this test particularly in the longitudinal direction where the phantom exterior surfaces are parallel to the imaging plane and are hence subject to volume averaging effects. Spatial information from the MVCT image can be deduced using the cursor position readout function available in the software. The use of a "fine" scan, i.e., a nominal slice thickness of 2 mm, is recommended for this scan. On the MVCT image, the orientation of the phantom should be correct. The MVCT images themselves should be free of unacceptable reconstruction artifacts. A minimum scan length of 20 cm is recommended for this test to approximate a typical scan length that is used in clinical routine. The dimension of the embedded objects or distances between fiducial markers as measured in the MVCT image should be within 2 and 1 mm of the physical distances for non-SRS/SBRT and SRS/SBRT treatments, respectively. The recommended test frequency and tolerances are in accord with those recommended in TG-142.

The accurate reconstruction of the MVCT image in terms of dimension and orientation should also be tested after sys-

tem maintenance work that can affect the hardware or software components that relate to the imaging system.

VI.B.1.b. Imaging/treatment/laser coordinate coincidence. The coincidence between the treatment and imaging coordinate system should be tested for any IGRT system. The meaning of this test changes somewhat for systems that use the treatment beam for image acquisition such as the tomotherapy MVCT system. While the beam source is identical for MVCT-based systems, the image acquisition, reconstruction, and registration involves hardware and software components that could induce discrepancies in the coordinate coincidence. It is therefore recommended to perform, on an annual basis and after software upgrades, a phantom-based end-to-end test of the image registration and treatment chain. For this test, a phantom will undergo the same chain of events that a patient would undergo. The phantom is imaged, a plan is generated in the TPS, MVCT imaging is used to check the phantom alignment, and finally the phantom is treated. The dose distribution within the phantom is tested for accuracy to establish image and treatment coordinate coincidence.

The phantom needs to contain either a film-based dosimeter or some other means of extracting a dose distribution for comparison with the dose distribution calculated in the treatment planning software. For example, ion chamber or diode arrays allow a direct measurement of the dose distribution in the phantom. Similarly, the vendor supplied Virtual Water™ phantom allows the placement of a film in the coronal or sagittal plane, and this phantom can be used for this test. In this case, the delivered dose distribution should be registered relative to the phantom. This registration can be performed within the TomoTherapy DQA panel with the aid of the "General" registration tool available in the DQA analysis panel. This registration tool allows a film registration that is based on any two points that can be identified on the film and in the CT image. Alternatively, the dose plane can be exported from the treatment planning system and the registration can be performed using third-party software. This test assesses the combined accuracy of the image registration and dose delivery process. A similar test is described in the literature by Soisson *et al.*[29] The tolerance should accommodate geographic uncertainties in the image registration and dose calculation. If each geographic uncertainty is assumed to be on the order of a voxel dimension or less, the tolerance of this test can be calculated by summing the two uncertainties in quadrature. Recommended tolerances for the treatment and imaging coordinate coincidence is 2 mm for non-SRS/SBRT and 1 mm for SRS/SBRT treatment machines. The imaging parameters and dose calculation grids may need to be chosen accordingly.

The annual test checks coincidence of the treatment and imaging system coordinates. A simultaneous test of the green laser system coincidence with the imaging system allows the establishment of the green laser system as a reference for daily and monthly consistency tests. This coincidence can be verified by checking that, post image registration, the green laser position on the phantom is in agreement with the intended position as indicated in the treatment planning system. When this test is performed, it must be kept in mind that the couch height may sag if a phantom is aligned at the virtual isocenter and is then moved to the treatment plane. Typically, the couch sag is on the order of 3 mm if vendor supplied cylindrical Virtual Water™ phantom is positioned on top of the couch. To avoid this offset, the phantom location with respect to the green laser should be checked at the treatment plane. Recommended tolerances for this test are 2 mm for non-SRS/SBRT and 1 mm for SRS/SBRT treatment machines.

The use of the green laser system as a surrogate is convenient since its operation is independent of the TomoTherapy machine operation and its position is thus not affected by the machine software or hardware upgrades.

On a daily basis, it is recommended to test the accurate location of the reconstructed image with respect to the green laser system to test the accurate location of the image coordinates with respect to the treatment coordinate. For this test, an object, i.e., a phantom with a high contrast object, is aligned with the red or green laser system and is scanned. The location of the object in the reconstructed MVCT image should agree with the actual location of this object with respect to the stationary green laser system. The tolerance for this test is 2 mm for non-SRS/SBRT and 1 mm for SRS/SBRT treatments. The use of the fine MVCT scan mode is recommended. A daily test of the treatment and imaging coordinate system coincidence with the given tolerances is in accord with recommendations made in TG-142.

Since accurate MVCT to kVCT image registration relies on accurate MVCT image localization, the above coincidence can be verified during the image registration test described in Sec. VI B 1 c.

VI.B.1.c. Image registration and alignment (position/repositioning). It is recommended to test the accuracy of the image registration and alignment process on a daily basis with a position/reposition test. The creation of a "phantom" patient plan can be used to test multiple aspects of the system. For example, a phantom that is intentionally and reproducibly misaligned prior to MVCT imaging can be scanned and registered to monitor the functionality and consistency of the image guidance process. A visual inspection of the image for image artifacts can be done at the same time. The image registration process should be reproducible to within 1 mm for phantoms that contain a high contrast object. Use of the fine scan option is recommended. The post registration positioning process should also be executed and actual couch and red laser shifts should match the intended shifts within 1 mm. The vendor supplied cylindrical Virtual Water™ phantom can be used for this test. The final, postregistration and alignment, positioning of the phantom should be accurate with respect to the green laser to within 1 mm. A daily position/repositioning test with identical tolerances is recommended in TG-142. An example phantom plan that tests, among other aspects, the consistency of the image registration and alignment process is described in Appendix D.

VI.B.2. Image quality tests

Image quality and dosimetry tests are recommended to quantify the initial performance of the system and to monitor this performance periodically. Quantitative tests at the time of machine acceptance allow the user to judge the performance of their system relative to recommended values. Periodic monitoring allows the user to quantify degradations in imaging parameters.

Image degradation could indicate suboptimal performance of the beam collimation, MVCT detector system, or variations in the MVCT beam with target wear. The accuracy of the primary y-jaws in defining the MVCT slice width in the longitudinal direction can influence the patient dose. If the fan beam is wider than intended, unnecessary dose will be delivered to the patient. The appearance of ring artifacts in the image points to a malfunction in the detector system. The Hounsfield unit (HU) to electron density conversion can also vary with target wear.

The image noise, uniformity, spatial resolution, contrast, and the MVCT dose are recommended for monitoring. The CT number reproducibility and image uniformity are essential if the MVCT images are used for dose calculations. Accordingly, the monthly MVCT QA protocol will vary with the intended MVCT use. Monthly tests of the image quality are in accord with TG-142 recommendations.

VI.B.2.a. Random uncertainty in pixel value (noise). To test image noise, an image of a water or water-equivalent uniform phantom can be used. The noise can be assessed by calculating the standard deviation σ_{CT} of the HUs in a region-of-interest (ROI). Noise is expressed relative to the linear attenuation coefficient of water μ_{water} and is corrected for the contrast scale (CS) of the scanner.[22] Hence, the

$$\text{Noise} = \sigma_{CT} \times \text{CS} \times 100/\mu_{water} \tag{9}$$

where

$$\text{CS} = (\mu_{polycarbonate} - \mu_{water})/(\text{HU}_{polycarbonate} - \text{HU}_{water}). \tag{10}$$

Using the above methodology noise values of 3.7–3.8 have been published for MVCT images.[30] This corresponds to a standard deviation of about 35–36 HU in a homogeneous water bath. When selecting the region-of-interest, the user should avoid areas of known image artifacts such as the "button" artifact that is frequently seen in the center of MVCT images. The button artifact is a region of enhanced density that is about 10 mm in diameter. It is an artifact of the rapidly changing detector response in the central region of the detector array.

It is recommended to determine the noise in the MVCT image using a cylindrical uniform phantom with a diameter of at least 20 cm. The vendor supplied cylindrical Virtual Water™ phantom contains a uniform section that can be used to determine the image noise. It is recommended to monitor the noise level on a monthly basis. The vendor does not issue a recommendation for acceptable noise levels and the acceptability of the measured noise level is at the user's discretion. Typical noise levels in the central region of the MVCT image are around 50–70 HU (one standard deviation) while lower values (i.e., 25–35 HU) can be expected in the periphery of the image.

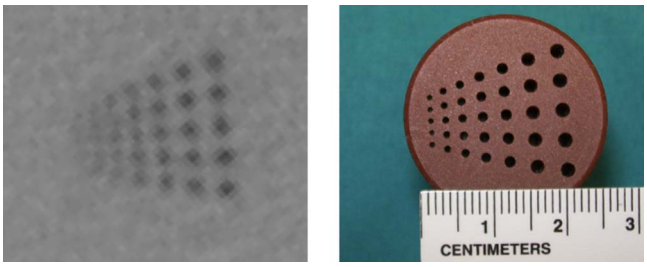

FIG. 20. MVCT image of the high contrast resolution plug that is shown on the left. The largest hole is 2 mm in diameter and the diameter is reduced in 0.2 mm steps for the smaller holes, i.e., the smallest hole has a diameter of 0.8 mm.

VI.B.2.b. Image uniformity. The uniformity can be assessed by measuring the average HU in smaller ROIs (about 5 mm in radius) that are located in the center and periphery of the phantom. The largest difference between any peripheral HU and the central HU is determined.

It is recommended to determine the uniformity in the MVCT image using a cylindrical uniform phantom with a diameter of at least 20 cm. The vendor supplied cylindrical Virtual Water™ phantom contains a uniform section that can be used to determine the image uniformity. It is recommended to monitor the image uniformity on a monthly basis.

If the MVCT image is used for dose calculation, the largest HU difference between the peripheral and the central ROIs should be less than 25 HU. A 25 HU difference in water would translate to a 2.5% variation in the calculated density of water.

VI.B.2.c. Spatial resolution. The spatial resolution can be measured with a high contrast hole pair test pattern. TomoTherapy provides a resolution plug that can be used for this test. This plug can be inserted into the vendor supplied cylindrical Virtual Water™ phantom. Alternatively, the resolution insert of an AAPM CT Performance Phantom (Cardinal Health, Hicksville, NY) or any similar spatial resolution insert can be used for this test. A monthly check of the MVCT image resolution should be performed. Figure 20 shows an MVCT image of a high contrast resolution test plug.

Visual inspection of a hole pattern indicated that MVCT images that are reconstructed with the typical 512×512 pixel matrix allow the resolution of a 1.25 mm high contrast object.[30] The vendor specifies a minimum resolution of a 1.6 mm high contrast object.

VI.B.2.d. Contrast. The low contrast visibility can be measured by inserting various density test plugs supplied by the vendor in the vendor supplied cylindrical Virtual Water™ phantom. On a monthly basis, the visibility of the identical test plugs can be checked. This test relies on the operator and is subjective in nature. However, a significant loss in contrast resolution will be detectable. Figure 21 shows an MVCT scan of the Virtual Water™ phantom that is loaded with test plugs of varying densities.

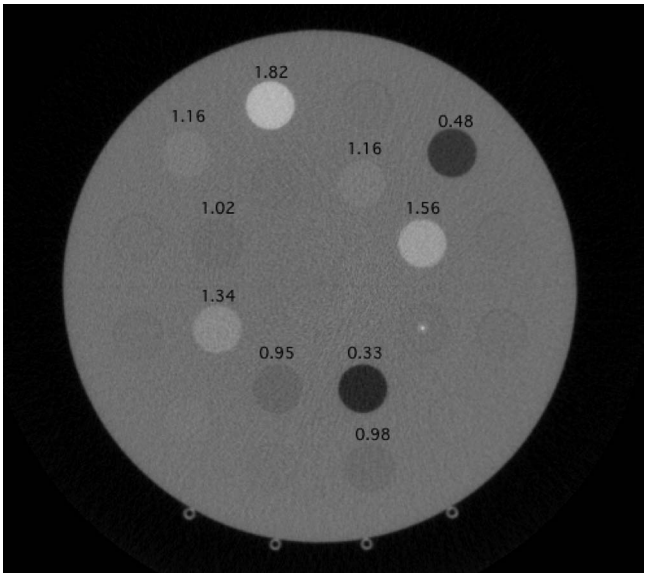

FIG. 21. MVCT image of the Virtual Water™ phantom loaded with various test plugs for a contrast and spatial resolution test. The numbers state some of the nominal plug densities in g/cm^3.

VI.B.2.e. CT number to density calibration. The relationship of MVCT number to electron or mass density is different from that observed in kVCT scanners. This is due to the difference in physical interaction probabilities in the two beams. In the megavoltage energy range, Compton interactions are dominant even in high Z materials. Consequently, the MVCT number to physical density calibration table is expected to reflect a linear relationship.

TomoTherapy has a commercial software package called "PLANNED ADAPTIVE" that facilitates the use of MVCT images for retrospective dose calculations to evaluate the dose distribution in the anatomy of the day. If MVCT images are used in this manner, a MVCT to density calibration must be commissioned and the reproducibility of the HU calibration should be monitored on a monthly basis. Similarly, if MVCT images are used for treatment planning, an accurate HU calibration must be used.

To commission the use of MVCT images for dose calculations, a commercial CT number calibration phantom can be used. The vendor supplied cylindrical Virtual Water™ phantom contains Virtual Water™ density plugs that can be exchanged with different density plugs for this purpose. A set of density plugs ranging from lung to bonelike densities is available from TomoTherapy. A MVCT scan of the calibration phantom is obtained and a MVCT number to density table can be established. The TomoTherapy TPS expects HU calibrations in terms of mass density rather than the more common relative electron density. These tables are called image value-to-density calibration tables (IVDTs) in the TomoTherapy TPS. An IVDT editor is available to commission and edit the IVDTs. After the IVDT is commissioned, its accuracy can be tested by recalculating the dose distribution of a phantom plan in the MVCT image of the phantom. Any rigid phantom, e.g., the vendor supplied cylindrical Virtual Water™ phantom can be used for this test. The original kVCT-based dose distribution should agree with the MVCT-based dose distribution. The PLANNED ADAPTIVE software facilitates a dose volume histogram comparison. The original and recalculated DVH should agree to within 2%.

If MVCT images are used for dose calculations, the reproducibility of this calibration curve should be monitored on a monthly basis with a subset of density plugs that cover lung, bone, and waterlike densities. The vendor supplied cylindrical Virtual Water™ phantom loaded with the appropriate density plugs can be used for this test. Any uncertainty in the HU calibration translates into dosimetric uncertainties in the MVCT-based dose calculation. The dosimetric impact of HU variations depends on what part of the calibration curve is affected. A shift in the water-equivalent HU has a larger impact than a shift in the bone equivalent HU since a typical patient image contains more water-equivalent density material than bonelike materials. Calibration curves that differed by 20 HU near water-equivalent densities and by up to 50 and 80 HU in lunglike and bonelike densities resulted in dosimetric differences of typically 2% or less for tomotherapy treatment plans.[31] Monthly HU calibration tests should test that the HU for water-equivalent materials varies by less than 30 HU and that lung and bonelike materials result in HUs that are within 50 HU of the nominal value established at time of machine acceptance.

VI.B.3. MVCT dosimetry

A multiple slice average dose (MSAD) measurement can be performed to measure the dose in phantom and to check the consistency of the imaging dose over time. Measurements are obtained with a calibrated ionization chamber that is located at a point of interest in a phantom, such as the vendor supplied Virtual Water™ phantom described in Sec. II. The scan ranges should cover the complete phantom. The dose measured at the ionization chamber location includes dose that is accumulated while the sensitive chamber volume is imaged as well as scatter dose accumulated when the neighboring slices are imaged. A simple cylindrical phantom or test plug that accommodates a calibrated ionization chamber such as a Farmer or an A1SL chamber can be used. The chamber specific TG-51 calibration factor can be used to convert the charge to dose. No adjustments for the image beam quality or irradiation conditions is recommended since the MVCT dose does not need to be measured with the same accuracy as the treatment dose.

The imaging dose will depend on the selected imaging mode and phantom but for the vendor supplied cylindrical Virtual Water™ phantom that is imaged in the "NORMAL" mode, a MSAD dose of 1–3 cGy can be expected.[24] Since the imaging beam is in the megavoltage range and the image is acquired in a helical fashion, the imaging dose is fairly uniform and the position of the ion chamber within the phantom is not critical. The same position should, however, be used for the consistency tests. It is recommended to monitor the imaging dose on a quarterly basis. While TG-142 recommends an annual measurement of the imaging dose a more frequent measurement is recommended for tomotherapy ma-

chines since MVCT images tend to be acquired on a frequent, i.e., daily, basis for each patient. Unexplained increases in the MVCT dose should be investigated.

VI.B.4. Image export for analysis

The analysis of MVCT images in terms of Hounsfield units cannot be done conveniently with the standard TomoTherapy software. For example, the TomoTherapy software has no tools to select a ROI for the calculation of mean HU and their standard deviation. To facilitate the analysis of MVCT images, it is therefore recommended to export the MVCT image from the TomoTherapy database and use third-party software for analysis. Using the DICOM export feature in the TomoTherapy software, it is possible to send MVCT images to a DICOM receiver. The Image-Guided Therapy QA Center (ITC) at Washington University in St. Louis supplies a convenient and free-of-charge DICOM receiver software package (DICOMpiler) (http://itc.wustl.edu/DICOMpiler/index.htm) that can be installed on a PC. Once exported, any image analysis software package [e.g., IMAGEJ from the National Institute of Health (NIH) (http://rsb.info.nih.gov/ij/)] can be used to analyze the HU distribution in a region-of-interest. Alternatively, DICOM export to a third-party treatment planning system can be investigated since appropriate image analysis tools may be available within these systems.

VII. TREATMENT PLANNING FOR HELICAL TOMOTHERAPY

VII.A. Introduction

The AAPM TG-53 report describes the QA guidelines for clinical 3D conformal radiotherapy treatment planning.[32] Not all of the issued guidelines apply to helical tomotherapy IMRT treatment planning, however, many aspects of these guidelines, e.g., the geometric tests of the TPS directly apply. Other aspects, such as the dosimetric verification of the TPS, apply but have to be adjusted to account for the specific workings of the TPS. In addition, for IMRT plans it is standard to check individual patient plans for accuracy. The intent of this chapter is to describe the treatment planning QA tests and their frequencies.

VII.A.1. Unique aspects of helical tomotherapy treatment planning

Since all TomoTherapy planning systems contain a common beam model, the traditional commissioning tasks of beam data entering and beam modeling do not apply to the tomotherapy planning system. There are no tools available in the treatment planning system to view the beam data that is used by the beam model. There are, however, two MLC-specific data files that are used by the planning system. These data files contain leaf latency and leaf specific fluence output data. In addition to these MLC-specific files, each machine has a specific set of y-jaw fluence output factors. These y-jaw fluence output factors specify the fluence of the 2.5 and 1.0 cm treatment slice fields relative to the 5.0 cm treatment slice field output. The fluence output for the 5 cm treatment slice width is a common value used by all TomoTherapy treatment planning systems.

After machine acceptance, the on-site physicist is left with site-specific tasks such as the generation of a kVCT scanner specific CT number to mass density calibration curve and the setup of connectivity of the helical tomotherapy TPS to external hardware. In the TomoTherapy TPS, Hounsfield units are calibrated against mass density rather than the more common relative electron density.

TomoTherapy's Hi-ART II TPS is exclusively used for planning. No other commercial TPS is available to generate treatment plans for delivery with TomoTherapy machines. There are a number of unique aspects of this TPS that are either due to the unique treatment delivery or are due to the specific working of this TPS. An understanding of these aspects is in the interest of treatment plan quality.

Due to its unique treatment delivery technique, unique planning parameters need to be chosen during the generation of a helical tomotherapy plan. For each plan, the treatment slice width, pitch, and modulation factor need to be selected.

The treatment slice width is the fan-beam width that is defined by the collimating y-jaws in the longitudinal direction at isocenter. Typically, three commissioned treatment slice widths (1.0, 2.5, and 5.0 cm) are available for selection.

The pitch value is defined as the ratio of the couch travel per gantry rotation to the treatment slice width and it is recommended to be less than 1. To increase dose homogeneity, pitch values less than 0.5 are typically used.[33] For off-axis targets, dose heterogeneities due to beam divergence and the cyclic nature of rotational beam delivery are possible. This "thread" or ripple effect increases with the treatment slice widths, pitch values, and off-axis distance.[34] An empirical study of this effect showed that for all treatment slice widths, the relationship between the size of the thread effect and the pitch contains minima at pitch values equal to $0.86/n$, where n is an integer.[34] For example, for a 2.5 cm treatment slice width and a pitch value of 0.287, the thread effect has a value of about 1% (peak-to-trough) at an off-axis distance of 5 cm. Changing the pitch value to 0.5 increases the thread effect to about 3% for the same conditions. However, the thread effect has little clinical impact for targets that are located on-axis.

If the dose per fraction is significantly higher than 2 Gy it may be necessary to reduce the pitch value to about 0.2 or less. The delivery of a higher dose requires the gantry to rotate slower and this may conflict with a required minimum gantry rotation speed of one rotation per minute. A reduction of the pitch value means that the target voxel is within the beam plane for more gantry rotations. This allows the gantry to rotate faster and enables the delivery of higher doses per fraction.

The modulation factor is defined as the longest leaf opening time divided by the average of all nonzero leaf opening times. The longest leaf opening time is significant because it determines the gantry rotation speed that is used during the delivery. The modulation factor that the user selects in the planning software is the maximum allowed modulation factor that is available to the optimization software. Often, the

final treatment plan has smaller modulation factors. The final modulation factor, called the "actual MF," is listed on the plan printout. A higher modulation factor may improve the plan quality and higher MFs are typically used for more complex target volumes. Typically, user selected modulation factors range from 1.5 to 3.5.

Treatment slice width, pitch, and modulation factor play important roles in the quality of the plan as well as the treatment time. The selection of a larger treatment slice width reduces the treatment time but may reduce dose conformity in the superior-inferior dimension. The selection of a smaller pitch value does not necessarily increase the treatment time since the gantry rotation speed is variable and can range from 15–60 s per rotation. Starting with the TomoTherapy software release 4.0, the maximum gantry speed will change from 15 to 12 s per rotation. A smaller pitch allows a faster gantry speed since a given voxel will experience more gantry rotations and less dose per rotation needs to be delivered. However, if the gantry is rotating at its maximum speed, a smaller pitch may increase the treatment time because the leaves are then forced to stay closed for a longer fraction of time. If the gantry rotation speed is reported to be at its maximum the user may wish to increase the pitch to prevent this loss of treatment efficiency.[35] A reduction of the modulation factor typically increases the gantry rotation speed and reduces the treatment time. However, this is only true if the gantry is not already rotating at its fastest speed. Similarly, an increase in modulation factor may not necessarily decrease the gantry rotation speed.

Once the plan parameters are selected, the dose distribution for each beamlet that passes through the target is calculated. The number of beamlets for a given plan depends on the slice width, pitch values, target volume, and shape. The beamlet calculation can be batched. The dose calculation engine uses the convolution/superposition method.[36] Once this beamlet calculation step is completed, the optimization process begins. A least square optimization method is used to optimize the objective function.[33]

Unlike conventional linear accelerators, helical tomotherapy treatments are terminated by time. The treatment planning system assumes a constant dose rate (about 850 cGy/min at a depth of 1.5 cm with an SSD of 85 cm and a 5×40 cm^2 static field). During the final dose computation and creation of the leaf control sinograms, the helical tomotherapy planning system uses measured MLC leaf latency data to determine the final programmed leaf opening times. At this final dose calculation, leaf opening times shorter than 20 ms are deleted from the control sinogram since they are too small in relationship to the actual leaf transition times. The final dose calculation reflects these changes and therefore it is possible to observe slight changes between the planned and final DVHs. The plan approval should be based on this final dose distribution.

Upon import into the helical tomotherapy system, the planning CT data set is typically down-sampled to an axial grid of 256×256 voxels. However, if the imported CT data set is extraordinary large, the user can choose to down-sample the CT data set to 128×128 voxels. The CT slice width is maintained. "Coarse," "normal," and "fine" calculation grids are available in the helical tomotherapy planning system. Dose calculation in fine mode results in a dose calculation grid that equals the imported CT data grid; normal and coarse modes result in dose calculations for every 2×2 or 4×4 imported CT voxels in the axial image, respectively. A coarser calculation grid may compromise the accuracy of dose volume histograms, particularly when the structures are small. Clinical significance of this may depend on the importance of the critical structures, their location relative to the PTV volumes, and the dose gradients within the structure. A finer dose calculation grid requires more computation time. The dose computation time scales directly with the number of voxels.

A collection of tomotherapy-specific treatment planning tips is located in Appendix F.

VII.B. Periodic quality assurance

Periodic geometric and dosimetric validation tests are recommended. Due to the system's complexity and uniqueness, independent dose calculation is nontrivial. The development of an independent dose calculation algorithm was recently explored by Gibbons *et al.*,[37] however, more commonly a dosimetric verification of the patient plan by measurement is performed.

VII.B.1. Geometric validation tests

TG-53 supplies guidance in regard to the image data import.[32] CT parameters such as pixel dimension and slice thickness should transfer correctly to the TPS. The image orientation (left-right, head-foot) must be correct. Text information about the patient orientation such as head-first-supine must transfer correctly from the CT scanner to the TPS. Image grayscale values must also transfer correctly. Most TomoTherapy users import the CT data into a third-party TPS system for contouring. The contours and CT data are then sent from this third-party system to the TomoTherapy TPS. Any test on the CT import should use the same route. CT scans of well defined phantoms, e.g., the vendor supplied cylindrical Virtual Water™ phantom, can be imported via the typical clinical workflow to the TPS to verify CT orientation, dimensions, grayscale values, and attached text data. The phantom dimension in the tomotherapy TPS should be within a kVCT voxel dimension of the physical dimension of the phantom. The accompanying structure set must transfer correctly from the third-party planning system to the TomoTherapy planning system. The location, dimension, and orientation of the structure set in relation to the kVCT images should be correct.

The geometric validation tests should be performed annually and after updates on any system that is involved in the CT acquisition and transfer process.

It should be kept in mind that the helical tomotherapy system down-samples the planning CT data set to 256×256 voxels. The associated structure set is not down-sampled upon import to the TomoTherapy system.

VII.B.2. Dosimetric validation tests

While the dosimetric commissioning tests contained in TG-53 may not directly apply to the testing of the tomotherapy system, the overall goal, i.e., testing of the dosimetric accuracy, applies to the tomotherapy TPS. Phantom based end-to-end tests are well suited to perform dosimetric verification tests. In these tests, phantoms are treated like patients in the sense that they undergo the same imaging, contouring, planning, and plan delivery steps that patients would undergo.

For dosimetric verifications, phantoms must be used that allow the measurement of dose with calibrated ionization chambers. Please refer to Sec. V B 5 for a discussion of acceptable ion chambers and specific correction factors for rotational tomotherapy deliveries. The standard cylindrical Virtual Water™ test phantom that is supplied with each treatment unit is well suited for the dosimetric verification tests. In this phantom, thimble ionization chambers (the vendor supplied cylindrical Virtual Water™ phantom is designed to accommodate A1SL chambers that are commercially available from Standard Imaging Inc., of Middleton, WI) can be placed at multiple locations.

Plans designed to treat on-axis and off-axis cylindrical targets should be generated for each commissioned slice width. A normal dose calculation grid should be used for the dose calculation. Targets should have volumes that are significantly larger than the sensitive volume of the ionization chamber. At a minimum, two targets, one centered at the center of rotation as indicated by the stationary green lasers and one off-axis target, should be treated in one plan or two separate plans. The AAPM Task Group Report 119 on "IMRT commissioning: Multiple institution planning and dosimetry comparisons" has produced a set of test plans and the physicist may want to review this document for guidance.[38]

There is no fundamental difference between the plans generated for the dosimetric verification and the plan generated for the pcsr-field calibration in Sec. V B 5 b and for the largest commissioned slice width the same plan can be used for both purposes.

Multiple point dose measurements should be performed in high and low dose regions. Dose gradient regions can be verified with multiple point dose measurements or planar dosimeters such as film or detector arrays. The acceptability criteria for dosimetric verifications are debated in the community. TG-53 lists dosimetric criteria but clarifies that these criteria are "collective expectation" values rather than requirements.[32] For 3D TPS systems, Van Dyk[39] listed acceptability criteria of 3% of the reference dose for high and low dose regions with low dose gradients and a 3 mm spatial agreement in high dose gradient regions. These values do not apply to areas of dose build-up or build-down. The recent TG-119 report provides helpful benchmark data that can be consulted for comparison when commissioning IMRT systems. In the TG-119 Report, a 3%/3mm gamma criteria were used for the evaluation of planar dose distributions.

Acceptability criteria for IMRT plans are currently formulated by the International Commission on Radiation Units and Measurements (ICRU) and will be published in a forthcoming ICRU report. Until the publication of this report, the Task Group recommends the use of 3%/3mm criteria for the dosimetric evaluation of the tomotherapy system. For the generated tomotherapy plans, point dose measurements should agree with the calculated dose to within 3% of the prescription dose or satisfy a 3 mm distance to agreement criterion. To evaluate the dosimetric pass rates the benchmark data provided by TG-119 can be consulted.

Ideally, a set of non-homogeneous phantoms should be available for testing prior to the start of patient treatment. Furthermore the verification of the calculated dose in regions other than unit density tissue is desirable. Several commercial phantoms exist for this purpose. However, in-house phantoms can be assembled to serve this purpose.

The dosimetric verification of the TPS should be performed after TPS software maintenance and annually.

VII.B.3. Clinical treatment plan QA

Once the planning system is used clinically each patient plan needs to be double checked for accuracy. Since no commercial solution for independent recalculation of helical tomotherapy dose distribution exists, current practice is to calculate each individual plan in a phantom geometry such that it can be dosimetrically verified by measurement. This current practice may evolve over time and alternative test procedures may be developed to replace the current one.

In the helical tomotherapy literature, dose recalculation of the treatment plan into a phantom geometry is called a DQA procedure. Tools to facilitate the DQA planning and analysis are integrated in the TomoTherapy planning software package. The DQA process requires that a CT scan of the phantom is imported into the tomotherapy planning system. After the calculation of the dose distribution in the phantom, point

TABLE II. Recommendations and tolerance limits for daily quality assurance procedures.

Daily test	Purpose	Tolerance limit	Report section
Output—Rotational or static	Consistency	3%	V.B.2.d
Image/laser coordinate coincidence	Accuracy	2–1 mm (non-SRS/SBRT-SRS/SBRT)	VI.B.l.b
Image registration/alignment	Accuracy	1 mm	VI.B.l.c
Red laser initialization	red=green laser	1.5–1 mm (non-SRS/SBRT-SRS/SBRT)	V.B.4.b

doses and planar dose distributions can be compared to measurements. A planar dose distribution can be exported from the tomotherapy system and this feature can be used for comparison with diode or ionization chamber arrays. Van Esch *et al.*[40] reported the use of an ionization chamber array for the dosimetric verification of tomotherapy plans. The use of a device that incorporates two orthogonal diode arrays for tomotherapy IMRT QA is reported by Guerts *et al.*[41]

It should be understood that the DQA plan verification does not test all aspects of the calculated treatment plan in the patient anatomy. For example, an incorrect mass density table could be applied during the patient plan calculation. This error will not be detected in a DQA procedure. Similarly, the correct replacement of the CT couch with the tomotherapy couch in the patient plan is not tested in the DQA process.

Most users currently use the vendor supplied cylindrical Virtual Water™ phantom for the patient plan verification and this is an acceptable verification procedure. In this process, a single point dose is measured with an ionization chamber and a single 2D dose distribution is measured with film. The measured ionization chamber points should be within 3% of the dose calculated with the TPS. If the measured ionization chamber point differs by more than 3% but less than 5%, it is recommended that the physicist investigate the discrepancy. At the discretion of the physicist and attending physician, treatment can be continued. If the discrepancy exceeds 5%, a thorough investigation is recommended prior to patient treatment. During the process of generating a DQA plan, the requested phantom position can be changed in the TPS and care should be taken to position the phantom such that the ionization chamber point is in a high dose and low dose gradient region. An ionization chamber measurement in such a region minimizes the problems associated with dose variations over the effective volume of the chamber. However, even larger low gradient dose regions are produced by the superposition of smaller fields and the user should be aware of uncertainties associated with small field dosimetry such as the potential lack of electronic equilibrium.

Analysis of the film plane is more revealing if the expected dose map contains both high and low dose regions. For planar dosimetry, a rectangle that encompasses the area within 5 mm from the phantom edge should be analyzed for a gamma coefficient.[42] It is the experience of the TG-148 Task Group that tomotherapy DQA plans that are calculated on a normal dose grid have typical gamma pass rate of at least 90% when a 3% dose difference/3 mm distance to agreement gamma criterion is used. The 3% dose difference is based on the prescription dose. If film dosimetry is used for the gamma analysis, the film dose can be scaled to match the ionization chamber reading in the target dose. While the TPS software facilitates the calculation of a gamma index, it

TABLE III. Recommendations and tolerance limits for monthly quality assurance procedures.

Monthly test	Purpose	Tolerance limit	Report section
Beam parameters			
Output—Static (IC)	Consistency	2%	V.B.2.d
Output—Rotational (IC)	Consistency with TPS	2%	V.B.2.d
Monitor chamber constancy	Constancy between monitor chambers	2%	V.B.2.d
Rotation output variation	Amplitude of variation	2%	V.B.2.d
Beam quality	Consistency with baseline	1% PDD_{10} or TMR_{10}^{20}	V.B.2.a
Transverse profile	Consistency with baseline	1% average difference in field core	V.B.2.b
Longitudinal profiles (each slice width)	Consistency with baseline	1% of slice width at FWHM	V.B.2.c
Alignment and Misc.			
Interrupted procedure	Agreement with uninterrupted Proc.	3%	V.B.4.a
Red laser movement	Correct movement	1 mm	V.B.4.b
Treatment couch	Digital readout versus actual movement	1 mm	V.B.4.c
Treatment couch	Level	0.5°	V.B.4.c
Treatment couch	Longitudinal motion alignment	1 mm	V.B.4.c
Treatment couch	Sag	5 mm	V.B.4.c
MVCT			
Geometric distortions	Dimension, orientation	2–1 mm (non-SRS/SBRT-SRS/SBRT)	VI.B.l.a
Noise	Monitor image quality	Consistency with baseline	VI.B.2.a
Uniformity	Monitor image quality	Consistency with baseline	VI.B.2.b
Spatial resolution	Monitor image quality	1.6 mm object	VI.B.2.c
Contrast	Monitor image quality	Consistency with baseline	VI.B.2.d
(if MVCT is used for dose calc.)			
Uniformity	Monitor image quality	25 HU	VI.B.2.b
HU (water test plug)	Monitor HU accuracy	within ±HU 30 of baseline	VI.B.2.e
HU (lung/bone test plug)	Monitor HU accuracy	within ±HU 50 of baseline	VI.B.2.e

TABLE IV. Recommendations and tolerance limits for quarterly quality assurance procedures.

Quarterly test	Purpose	Tolerance limit	Report section
Synchronicity			
Gantry angle	Correct and consistent	1°	V.B.3.a
Couch speed uniformity	Uniform	2% dose nonuniformity	V.B.3.b
Couch translation per gantry rotation	Synchrony	1 mm per 5 cm	V.B.3.c
MVCT			
Dose	Monitor image dose	Consistency with baseline	VI.B.3

does not currently allow the selection of a region of interest for analysis. Hence, the evaluation of the pass criteria requires export and analysis of the measured and calculated dose distributions with third-party analysis programs. At the discretion of the on-site physicist(s), a visual evaluation of the calculated gamma distribution may suffice.

If DQA results are outside the tolerance level, the clinical physicist needs to investigate. Initially, the phantom setup should be verified along with the correct extraction of the calculated point dose from the TPS. It should also be investigated if the ionization chamber measurement is in or near a high-gradient region. While this scenario should be avoided,

TABLE V. Recommendations and tolerance limits for annual quality assurance procedures.

Annual test	Purpose	Tolerance limit	Report section
Mechanical alignments			
y-jaw centering	Source to y-jaw alignment	0.3 mm at source	V.B.1.a
x-alignment of source	Source to MLC alignment	0.34 mm at source	V.B.1.b
y-jaw divergence/beam centering	Source alignment with axis of rotation	0.5 mm at iso	V.B.1.c
y-jaw/gantry rotation plane alignment	y-jaw alignment with axis of rotation	0.5°	V.B.1.d
Treatment beam field centering	Common center	0.5 mm at iso	V.B.1.e
MLC lateral offset	MLC alignment with center of rotation	1.5 mm at iso	V.B.1.f
MLC twist	Alignment with beam plane	0.5°	V.B.1.f
Beam parameters			
Beam quality (each slice width)	Agreement with model	1% PDD_{10} or TMR_{10}^{20}	V.B.2.a
Transverse profile (each slice width)	Agreement with model	1% average difference in field core	V.B.2.b
Longitudinal profiles (each slice width)	Agreement with model	1% of slice width at FWHM	V.B.2.c
TG-51 calibration	Calibration	1%	V.B.5
Misc.			
Axial green laser (distance and twist)	Nominal distance to iso	1 mm/0.3°	V.B.4.b
Sagittal/coronal green laser	Alignment with axis of rotation	±1 mm	V.B.4.b
MVCT			
Imaging/treatment/laser coordinate coincidence	accurate location of dose	2–1 mm (non-SRS/SBRT-SRS/SBRT)	VI.B.1.b
Treatment planning system			
CT data import			
Dimension of object in TPS	Agreement with physical dimension	1 kVCT voxel	IV.B.2
CT voxel dimensions	Correct transfer	Pass/fail	IV.B.2
CT orientation	Correct transfer	Pass/fail	IV.B.2
CT gray scale values	Correct transfer	Pass/fail	IV.B.2
Associated text info	Correct transfer	Pass/fail	IV.B.2
Structure set import			
Dimension of structure	Agreement with contouring software	1 kVCT voxel	IV.B.2
Location of structure	Agreement with contouring software	Pass/fail	IV.B.2
Orientation of structure	Agreement with contouring software	Pass/fail	IV.B.2
Dosimetric verification			
Point dose in low gradient area	Agreement with TPS	Within 3%	IV.B.3
Point dose in high gradient	Agreement with TPS	3%/3 mm	IV.B.3

TABLE VI. Recommendations and tolerance limits for quality assurance procedures post major component replacement.

After major component replacement test	Purpose	Tolerance limit	Report section
Magnetron/SSM			
Output—Static (IC)	Consistency	2%	V.B.2.d
Output—Rotational (IC)	Consistency with TPS	2%	V.B.2.d
Rotation output variation	Amplitude of variation	2%	V.B.2.d
Beam quality	Consistency with baseline	1% PDD_{10} or TMR_{10}^{20}	V.B.2.a
Transverse profile	Consistency with baseline	1% average difference in field core	V.B.2.b
Longitudinal profile	Consistency with baseline	1% of slice width at FWHM	V.B.2.c
DQA/phantom plan	Agreement with TPS	3%	VII.B.5
(if MVCT is used for dose calc.)			
HU (water test plug)	Monitor HU accuracy	within ±HU 30 of baseline	VI.B.2.e
HU (lung/bone test plug)	Monitor HU accuracy	within ±HU 50 of baseline	VI.B.2.e
Linac/target			
y-jaw centering	Source to y-jaw alignment	0.3 mm at source	V.B.1.a
x-alignment of source	Source to MLC alignment	0.34 mm at source	V.B.1.b
y-jaw divergence/beam centering	Source alignment with axis of rotation	0.5 mm at iso	V.B.1.c
Output—Static (IC)	Consistency	2%	V.B.2.d
Output—Rotational (IC)	Consistency with TPS	2%	V.B.2.d
Rotation output variation	Amplitude of variation	2%	V.B.2.d
Beam quality	Consistency with baseline	1% PDD_{10} or TMR_{10}^{20}	V.B.2.a
Transverse profile	Consistency with baseline	1% average difference	V.B.2.b
Longitudinal profiles (each slice width)	Consistency with baseline	1% of slice width at FWHM	V.B.2.c
DQA/phantom plan	Agreement with TPS	3%	VII.B.5
(if MVCT is used for dose calc.)			
HU (water test plug)	Monitor HU accuracy	within ±HU 30 of baseline	VI.B.2.e
HU (lung/bone test plug)	Monitor HU accuracy	within ±HU 50 of baseline	VI.B.2.e
y-jaw (actuators/encoders)			
y-jaw centering	Source to y-jaw alignment	0.3 mm at source	V.B.1.a
y-jaw divergence/beam centering	Source alignment with axis of rotation	0.5 mm at iso	V.B.1.c
y-jaw/gantry rotation plane alignment	y-jaw alignment with axis of rotation	0.5°	V.B.1.d
Treatment beam field centering	Common center	0.5 mm at iso	V.B.1.e
Longitudinal profiles (each slice width)	Consistency with baseline	1% of slice width at FWHM	V.B.2.c
Output—Static (IC)	Consistency	2%	V.B.2.d
Output—Rotational (IC)	Consistency with TPS	2%	V.B.2.d
Rotation output variation	Amplitude of variation	2%	V.B.2.d
DQA/phantom plan	Agreement with TPS	3%	VII.B.5
MLC			
x-alignment of source	Source to MLC alignment	0.34 mm at source	V.B.1.b
MLC lateral offset	MLC alignment with center of rotation	1.5 mm at iso	V.B.1.f
MLC twist	Alignment with beam plane	0.5°	V.B.1.f
DQA/phantom plan	Agreement with TPS	3%	VII.B.5

a small target volume may result in the chamber being placed in or near such a high gradient. If the target is considerably off-axis and the plan was generated with a large pitch value or slice width, the measurement point may be in an inhomogeneous area due to the thread effect. Volume averaging and distance to agreement techniques can be used judicially when DQA discrepancies are investigated.

A drift in the machine output can lead to unacceptable DQA results. A repeat of a previous or a standard DQA plan can be useful for this analysis. An analysis of the daily output checks could also be helpful. An adjustment of the machine output may be required. It is recommended that the physicist has a standard IMRT plan available for each treatment slice width. Phantom plans or previous DQA plans for representative clinical scenarios can be used for this purpose. These plans would have similarities in gantry speed, leaf opening times, etc., and a repeat of these plans may help to determine if the measured dose discrepancy is specific to a plan or uniform for all plans.

The use of short leaf opening times has been associated

with possible DQA discrepancies.[35] Shorter leaf opening times occur if plans use low pitch values. Planning with a higher pitch value (around 0.287 for a prescription dose of 2 Gy) will reduce this delivery uncertainty.

VII.C. MVCT-based treatment planning

Metallic implants cause fewer image artifacts in MVCT images compared to standard kVCT images. MVCT-based treatment planning can hence be of advantage for patients that have artificial implants and in whom regular kVCT artifacts hinder treatment planning.[43]

If MVCT images are used for treatment planning purposes, it is recommended that an up-to-date MVCT to mass density table be measured immediately before or after the patient planning image is acquired. This recommendation is based on the observation that the MVCT Hounsfield numbers are susceptible to changes in the imaging beam that are secondary to target wear and other factors that are still under investigation. It is also recommended to obtain a scan of the DQA phantom at the same time. This latter scan should be used in the DQA process of the MVCT-based treatment plan. The measured MVCT density table should be applied to the patient and DQA phantom MVCT images. Furthermore, it is recommended to contour areas of high density such as metallic hip implants and to prohibit beam entrance through these areas. This is done to avoid uncertainties in the beam attenuation calculations associated with high-density materials. These uncertainties have two sources: (1) The fluence attenuation tables have data up to a maximum density of 4 g/cm^3 and for higher densities the TPS defaults to using this maximum density and (2) the IVDT tables for MVCT images will need to be extended to high-density materials.

VIII. SUMMARY AND RECOMMENDATIONS

In this chapter, the QA aspects discussed in the previous chapters are summarized and arranged according to their recommended frequencies. Recommendations on what to QA after machine service work are also listed in the chapter for several service scenarios.

VIII.A. Daily

On a daily basis, the beam output should be monitored. The output consistency should be measured under static and/or rotational conditions. If the static output is monitored on a daily basis, the rotational output should be monitored on a weekly basis and vice versa. The correct initialization of the laser system should be checked. After the image registration, the automatic couch and red laser adjustment should be tested daily. It should be checked visually that the MVCT quality is consistent with that accepted at time of commissioning and that there are no gross artifacts in the image. It should be checked that the image registration process is operating consistently. An example procedure that combines several tests in one procedure is outlined in Appendix D. Table II summarizes the recommendations for daily QA. Standard safety tests are not included in this list. They should be performed per recommendations detailed in TG-142.[3]

VIII.B. Monthly

Monthly tests cover beam parameter consistency tests, MVCT tests and miscellaneous aspects. Table III summarizes the recommended tests and their tolerance limits. Standard safety tests such as interlock testing are not covered in the table but should be performed per recommendations detailed in TG-142.[3]

VIII.C. Quarterly

On a quarterly basis, the gantry angle and the uniformity of the couch movement should be tested. The synchrony between couch translations and gantry rotations should also be tested at this interval. The MVCT dosimetry should be done quarterly. Table IV summarizes the recommended tests and their tolerance limits.

VIII.D. Annual

Annual tests contain mechanical alignment, beam parameters, and miscellaneous test items. MVCT registration and an end-to-end test of the registration process should be performed as well as several treatment planning system tests. Table V summarizes the recommended tests and their tolerance limits.

VIII.E. Major component replacement

The replacement of major components necessitates QA tests. These tests obviously depend on the particular service issues. Recommended post service tests are discussed for several scenarios. Table VI summarizes the recommended QA test for four service scenarios.

Magnetron/solid state modulator (SSM): A replacement of the magnetron or SSM can change beam parameters such as output and beam energy. It is recommended that the user tests beam output, energy, and longitudinal as well as lateral profiles. The beam parameters only need to be tested for one slice width. It is the intent of these tests to check that the parameters are consistent with the baseline values. A repeat of the monthly QA procedures of these beam parameters should be sufficient to establish consistency with nominal values. If MVCT images are used for dose calculations, the monthly QA test for HU accuracy should be performed. Post service, a DQA or phantom plan should be checked and verified for agreement with calculations. This last step also forces the user to exercise all functions (imaging registration and treatment) that are used for regular treatments. This tests that the system is fully operational.

Linac or target: A replacement of the target requires a movement of the Linac during the process. The source alignment (Secs. V B 1 a, V B 1 b, and V B 1 c) needs to be tested post-target/linac replacement. In addition, all tests that are recommended post magnetron/SSM replacement should be performed post-target/linac alignment.

Y-jaw: Work on the y-jaws, actuators, or encoder necessitates a verification of the y-jaw alignment and longitudinal beam profiles. The jaw centering, divergence, and alignment with the rotation plane should be checked in addition to the treatment field centering. Longitudinal beam profiles should be collected and checked for agreement with the reference beam data. In addition to a beam output check, DQA or phantom plans should be checked for each commissioned slice width and verified for agreement with calculations.

MLC: Replacement of the MLC requires MLC alignment tests to be performed. The MLC lateral offset as well as the MLC twist should be tested. The vendor includes MLC-specific leaf latency data in the treatment planning system. It is not possible to adjust the leaf latency for a given MLC. Instead, the vendor will measure and update these data in the TPS after a MLC replacement. These data are used at the time of "Final Dose" calculation and therefore are only applied to plans that are generated subsequently. Existing plans are not altered. It is therefore recommended to repeat several DQA plans for existing patients to ensure that these are within acceptable tolerance. Plans with short leaf opening times may be more sensitive and should be included in the group of plans that is selected for this test. If DQA plans are out of tolerance the user may have to replan selected cases.

APPENDIX A: WORKSHEET A: HELICAL TOMOTHERAPY PHOTON BEAM CALIBRATION

1. Site data

Institution: _____

Physicist: _____

Date: _____

Accelerator: _____

Model & serial number: _____

2. Instrumentation

a. Chamber model: _____

Serial number: _____

Cavity inner radius (r_{cav}): _____ cm

Waterproof: yes ☐ no ☐

If no, is waterproofing ≤1 mm PMMA or thin latex?: yes ☐ no ☐

b. Electrometer model: _____

Serial number: _____

i. P_{elec}, electrom. corr. factor: _____ C/C or C/rdg

c. Calibration factor N_{D,W,Q_o}: _____ Gy/C (or Gy/rdg)

Date of report (not to exceed 2 years): _____

3. Measurement Conditions (choose step a. or step b.)

a. Static Beam Output (5 cm x 10 cm, measurement at 10 cm depth water equivalent)

i. Distance (SSD or SAD): _____ cm SSD ☐ or SAD ☐

ii. Field size: _____ cm^2

on surface (SSD setup): ☐ at detector (SAD setup): ☐

iii. Irradiation time: _____ min

b. Rotational Beam Output (8 cm diameter x 10 cm long homogeneous dose volume within a 30 cm diameter water equivalent phantom)

i. Axial collimation: _____ cm

4. Beam Quality

Measure beam quality specifier $\%dd(10)_{x(HT\ ref)}$ [FS=5 cm × 10 cm, 85 cm SSD, % depth-dose at 10 cm depth for curve shifted upstream by $0.6r_{cav}$]

Field size 5 cm x 10 cm on surface, SSD = 85 cm: yes ☐ no ☐

a. $\%dd(10)_{x(HT\ ref)}$: _____

Using the following equation or Figure 19 to determine $\%dd(10)_{x(HT\ TG\text{-}51)}$:

$$\%dd(10)_{x[HT\ TG\text{-}51]} = 1.35805 \bullet (\%dd_{(10)x[HT\ ref]})^3 - 244.493 \bullet (\%dd_{(10)x[HT\ ref]})^2 + 14672.98 \bullet \%dd_{(10)x[HT\ ref]} - 293479.4$$

b. $\%dd(10)_{x(HT\ TG\text{-}51)}$: _____

5. Determination of $k_{Q,Q_0} \times k_{Q_{msr},Q}^{f_{msr},f_{ref}}$

Chamber model used to get $k_{Q,Q_0} \times k_{Q_{msr},Q}^{f_{msr},f_{ref}}$: _____

a. $k_{Q,Q_0} \times k_{Q_{msr},Q}^{f_{msr},f_{ref}}$ [Table 1]: _____

6. Temperature/pressure Correction

a. Temperature: _____ ºC

b. Pressure: _____ kPa $\left[= \text{mmHg}\frac{101.33}{760.}\right]$

c. P_{TP}: _____ $\left[P_{TP} = \left(\frac{273.2 + 6a}{295.2}\right)\left(\frac{101.33}{6b}\right)\right]$

7. Polarity correction

M_{raw}^{+}: _____ C or rdg

M_{raw}^{-}: _____ C or rdg

a. M_{raw} (for polarity of calibration): _____ C or rdg

b. P_{pol}: _____ $\left[P_{pol} = \left|\frac{\left(M_{raw}^{+} - M_{raw}^{-}\right)}{2M_{raw}}\right|\right]$

8. P_{ion} measurements

Operating voltage = V_H: _____ V

Lower voltage V_L: _____ V

M^{H}_{raw}: _____ C or rdg

M^{L}_{raw}: _____ C or rdg

a. P_{ion} (V_H): _____ $\left[P_{ion}(V_H) = \left(1. - \frac{V_H}{V_L}\right) \Big/ \left(\frac{M^{H}_{raw}}{M^{L}_{raw}} - \frac{V_H}{V_L} \right) \right]$

If P_{ion}> 1.05, another ion chamber should be used.

9. Corrected ion. ch. rdg. M for msr or pcsr field:

$M_{corr} = P_{ion}P_{TP}P_{elec}P_{Pol}M_{raw}$ = [8a·6c·2b.i·7b·7a] = _____

10. Dose to water at 10 cm depth for Static Beam Output:

a. $D^{f_{msr}}_{w,Q_{msr}} = M^{f_{msr}}_{Q_{msr}} \bullet N_{D,w,Q_0} \bullet \left[k_{Q,Q_0} \bullet k^{f_{msr},f_{ref}}_{Q_{msr},Q} \right]$ = [9 · 2c · 5a] = _____ Gy

b. Dose/ min at 10 cm depth: _____ Gy/min [10a/3a.iii]

c. Clinical %*dd*(10) for SSD setup / 100: _____

or clinical TMR(10) for SAD setup: _____

Dose / min at d_{max}: _____ Gy/min [10b/10c]

11. Correction factor between conventional reference field and plan-case specific reference field

$k^{f_{pcsr},f_{msr}}_{Q_{pcsr},Q_{msr}}$: 1.003

12. Dose to pcsr field for Rotational Beam Output:

$$D^{f_{pcsr}}_{w,Q_{pcsr}} = M^{f_{pcsr}}_{Q_{pcsr}} \bullet N_{D,W,Q_o} \bullet \left[k_{Q,Q_o} \bullet k^{f_{msr},f_{ref}}_{Q_{msr},Q} \right] \bullet k^{f_{pcsr},f_{msr}}_{Q_{pcsr},Q_{msr}} = [9 \cdot 2c \cdot 5a \cdot 11] =$$ _____ Gy

APPENDIX B: NOTE ON CONTROL XML FILES AND CONTROL SINOGRAMS

Typically, the machine receives operating instructions via XML files that are generated at the end of the treatment planning process. To pass instructions to the machine independently of the treatment planning system requires that the user generate an XML file. Tools to generate XML files are included in the operator station software. These files contain, among others, instructions on gantry position, table movements, and MLC opening patterns. The vendor supplies a number of XML files and the associated binary MLC control files (control sinograms) that can be used to run some of the procedures detailed in this report. If the user wants to generate their own XML files, it is recommended to select an existing XML file and modify it according to the user's intentions. These files can be viewed, modified, and saved using the operator station software. Details of how to develop XML files can be found in the TomoTherapy documentation (Calibration Data Tool Guide, Version 3.X).

Embedded in the XML file is a reference to a binary file referred to as the control sinogram which controls the timing of the binary MLC leaves during treatment delivery. The control sinogram is a binary file with 64 columns. Each column contains a value ranging from 0.0 to 1.0. These values are normalized opening times for each leaf. Leaf opening times must be supplied for each leaf and projection. The sinogram files must therefore have a minimum number of rows that is equal to the number of delivered projections. The duration of each projection is defined elsewhere in the XML file.

APPENDIX C: RADIATION SAFETY

IMRT techniques have raised unique room-shielding concerns that are mainly due to increased workloads. In addition to room shielding, leakage concerns have been raised for some systems since the increased workload may affect the whole body doses that the patient receives.[44]

Shielding and leakage concerns specific to helical tomotherapy have been addressed in the literature.[45–49] The continuous rotation of the gantry complicates the traditional usage factor that accounts for the particular beam direction employed. Additionally, due to the exclusive IMRT treatment mode, the workload is significantly larger than with traditional accelerators. Workloads of 10^6 MU per week are often assumed for shielding calculations, which is about an order of magnitude greater than the workload for non-IMRT accelerators.[46] However, since helical tomotherapy was designed exclusively as an IMRT machine, extra shielding was designed into the accelerator head. This extra shielding is assembled around the linac to (i) protect the patient from unwanted exposure and to (ii) reduce linac leakage. In addition, a beam stop was added to the machine that provides over two orders of magnitude of primary beam attenuation. Continuous gantry rotation also serves to decrease the contribution of primary beam exposure since it limits the time any point is exposed to the primary beam. There is actually more exposure due to backscattered leakage radiation than due to direct primary radiation at 2 m from the isocenter. Due to differences in energy between primary and leakage radiation and different effective source positions, that ratio may change as a function of shielding wall distance and thickness. A final but significant advantage for room-shielding designs is that helical tomotherapy units only have a single nominal 6 MV beam energy.

Patient scatter is approximately the same as with all external beam radiation therapy since the patient integral dose is approximately the same regardless of the modality. The effect of the unique tomotherapy design is that backscattered leakage radiation dominates shielding concerns. Tomotherapy provides a site-planning guide which lists a polar plot of leakage levels versus distance and angle from the isocenter to assist in shielding design.

In general, helical tomotherapy units can safely be installed in most bunkers with standard-density concrete walls 3.5 to 4.0 ft thick. Of course, each proposed bunker must be extensively analyzed. Furthermore, goal exposure levels do vary according to the site specifics. To verify shielding requirements post install, access to an integrating survey meter is helpful.

Exposure due to scattered radiation at the door is similar to that of conventional machines. Radiation at the door consists mostly of scattered leakage radiation. As such, it is of much lower energy. McGinley[50] has calculated such scattered photon radiation to be less than 0.3 MeV. Therefore, a 1/4 in. lead liner in a wood door is usually more than sufficient for shielding. Exact entrance exposure is dependent on maze length and width and overall room size and geometry.

TomoTherapy, Inc. will soon offer a new product, "TomoDirect." This will allow the gantry to operate in a static gantry mode while the couch translates and MLC leaves modulate. This will decrease beam-on time for some treatments more suitable for nonrotating delivery. It is not yet known how TomoDirect will affect shielding requirements. Most likely, required shielding will only decrease because TomoDirect was designed to decrease beam-on time.

The unique features of the tomotherapy unit may conflict with certain local regulations such as regulations on field flatness and symmetry. Local regulations should be interrogated for possible conflicts. Regulatory exemptions may have to be applied for.

APPENDIX D: EXAMPLE OF DAILY TEST PROCEDURES

With the gantry at a static position the beam output can be tested. The rotational output (or integral dose) can be tested with a phantom patient plan. This procedure is generated in the TPS. During the plan generation, the movable red lasers can be intentionally offset from the alignment marks. The offsets should be similar to what is typically encountered in the clinic. A daily MVCT scan, registration, and alignment of this phantom then serves to test the laser functionality, image registration, and automatic couch alignment procedure. The final phantom position can be checked against the green laser system by marking the expected green laser projection on the

phantom. If the phantom is always placed in the same location on the couch (e.g., phantom position can be marked on couch), the consistency of the initial table readout is also tested. After alignment, the delivery of the correct dose can be verified, i.e., the rotational output can be tested. All tests can be done with the vendor supplied cylindrical Virtual Water™ phantom. However, some users have designed phantoms specifically for daily QA of TomoTherapy units.[7]

APPENDIX E: PATIENT ARCHIVES

The user can generate an archive of a patient plan at any time using the patient archiving tool integrated in the planning station or operator station software. This patient archive contains a wealth of information: Planning parameters, kVCT and MVCT images, planned MLC sinograms, recorded detector data sinograms, recorded monitor chamber signal, and more. Some of this information is stored in binary format in separate files that are part of the archive. Each patient archive contains an XML file that is labeled with the patient's name. This XML file contains numerical information (e.g., registration offsets) and provides the file names for the MVCT or detector sinogram files. The patient archive can then be searched for this file. A third-party XML viewer is recommended to view the XML file and third-party software, e.g., MATLAB (The MathWorks, Inc., Natick, MA), can be used to read, display, and analyze image or sinogram files. Detector data can also be extracted immediately after a procedure is completed using a tomotherapy quality assurance tool that is commercially available from the vendor.

APPENDIX F: TREATMENT PLANNING TIPS

Like other IMRT TPS, the helical tomotherapy planning system is driven by dose-based objectives, their associated penalties, and ROI-based weighting factors. For tumor or target volumes, minimum and maximum dose values and their respective penalties are used in addition to a DVH-based prescription point. Sensitive structure objectives are described by a maximum dose, a DVH-based constraint, and their respective penalties. However, it is important to recognize that in the helical tomotherapy TPS, the DVH-based prescription for one selected target structure is a hard constraint, which means that it is always met. The optimized treatment plan is scaled after each iteration to satisfy this DVH-based prescription dose.

The treatment planning system prompts the user to divide regions of interest into two groups: (i) Tumors and (ii) sensitive structures. If ROIs in the same group overlap, the voxels contained in the overlap region can only be assigned to one or the other structure for the purpose of plan optimization and dose volume histogram calculations. The overlap priority setting governs to which structure the voxel belongs. It is therefore possible that in the case of overlapping structures, the DVH statistics may not completely reflect the volume of interest. It is important that all involved parties understand this. However, in future software releases, the use of overlap priorities may change and the user needs to be aware how these priority settings are used in their current software release.

There are two sets of lasers used in helical tomotherapy planning and delivery. Fixed green lasers define a virtual isocenter that is nominally 70 cm away from the gantry (treatment and imaging beam) isocenter. A movable red laser system is used for patient positioning. During the treatment planning process, the red lasers can be requested to point toward the patient's setup marks. The physical movement of the red lasers in the treatment room is restricted to a maximum distance of about 20 cm from the green laser system at isocenter. The exact value depends on the particular laser placement in the room and is site-specific. During treatment planning, it is possible to request larger movements of the red laser system. However, these requests result in a hardware error interrupt (i.e., a nondeliverable procedure) once these plans are selected for treatment. This scenario can be avoided if a smaller laser separation is selected. The selected distance should allow for possible further red laser movements after image registration. The axial laser settings are most susceptible to this issue and the position of the axial green laser with respect to the patient can be adjusted in the planning system to alleviate this problem.

During treatment the patient is moved in the longitudinal (i.e., y) direction through the rotating fan-beam plane. The fan beam is used for treatment as soon as the superior target edge enters the beam plane and the treatment is completed only after the inferior target edge leaves the beam plane. Consequently, an area equivalent to the longitudinal dimension of the fan beam is exposed superior and inferior to the target volume. It is recommended that the treatment planning CT volume extends superior and inferiorly beyond the target volume by a length sufficient to include any irradiated volume. Taking beam divergence into account this is typically satisfied if the CT volume extends by a distance larger than two treatment slice widths.

[a]Conflict of interest: Dr. Gustavo Olivera is an employee of TomoTherapy, Inc. and has a financial interest in TomoTherapy, Inc. Dr. Olivera served as an industry consultant to this task group. Dr. John Balog owns TomoTherapy stock. Dr. Katja Langen holds a research agreement with TomoTherapy, Inc.
[b]Electronic mail: Katja.Langen@orlandohealth.com

[1]G. J. Kutcher *et al.*, "Comprehensive QA for radiation oncology: Report of AAPM Radiation Therapy Committee Task Group 40," Med. Phys. **21**(4), 581–618 (1994).
[2]R. Nath, P. J. Biggs, F. J. Bova, C. C. Ling, J. A. Purdy, J. van de Geijn, and M. S. Weinhous, "AAPM code of practice for radiotherapy accelerators: Report of AAPM Radiation Therapy Task Group No. 45," Med. Phys. **21**(7), 1093–1121 (1994).
[3]E. E. Klein, J. Hanley, J. Bayouth, F. F. Yin, W. Simon, S. Dresser, C. Serago, F. Aguirre, C. Ma, B. Arjomandy, C. Liu, C. Sandin, and T. Holmes, "Task Group 142 Report: Quality assurance of medical accelerators," Med. Phys. **36**(9), 4197–4212 (2009).
[4]T. R. Mackie, T. Holmes, S. Swerdloff, P. Reckwerdt, J. O. Deasy, J. Yang, B. Paliwal, and T. Kinsella, "Tomotherapy: A new concept for the delivery of dynamic conformal radiotherapy," Med. Phys. **20**(6), 1709–1719 (1993).
[5]J. Balog, T. Holmes, and R. Vaden, "A helical tomotherapy dynamic quality assurance," Med. Phys. **33**(10), 3939–3950 (2006).
[6]J. D. Fenwick, W. A. Tome, H. A. Jaradat, S. K. Hui, J. A. James, J. P. Balog, C. N. DeSouza, D. B. Lucas, G. H. Olivera, T. R. Mackie, and B.

R. Paliwal, "Quality assurance of a helical tomotherapy machine," Phys. Med. Biol. **49**(13), 2933–2953 (2004).
[7]S. M. Goddu, S. Mutic, O. L. Pechenaya, S. R. Chaudhari, J. Garcia-Ramirez, D. Rangaraj, E. E. Klein, D. Yang, J. Grigsby, and D. A. Low, "Enhanced efficiency in helical tomotherapy quality assurance using a custom-designed water-equivalent phantom," Phys. Med. Biol. **54**(19), 5663–5674 (2009).
[8]J. Balog, T. R. Mackie, D. Pearson, S. Hui, B. Paliwal, and R. Jeraj, "Benchmarking beam alignment for a clinical helical tomotherapy device," Med. Phys. **30**(6), 1118–1127 (2003).
[9]R. Jeraj, T. R. Mackie, J. Balog, G. Olivera, D. Pearson, J. Kapatoes, K. Ruchala, and P. Reckwerdt, "Radiation characteristics of helical tomotherapy," Med. Phys. **31**(2), 396–404 (2004).
[10]E. Sterpin, F. Salvat, R. Cravens, K. Ruchala, G. H. Olivera, and S. Vynckier, "Monte Carlo simulation of helical tomotherapy with PENELOPE," Phys. Med. Biol. **53**(8), 2161–2180 (2008).
[11]R. J. Staton, K. M. Langen, P. A. Kupelian, and S. L. Meeks, "Dosimetric effects of rotational output variations and x-ray target degradation on helical tomotherapy plans," Med. Phys. **36**(7), 2881–2888 (2009).
[12]K. M. Langen, S. L. Meeks, D. O. Poole, T. H. Wagner, T. R. Willoughby, O. A. Zeidan, P. A. Kupelian, K. J. Ruchala, and G. H. Olivera, "Evaluation of a diode array for QA measurements on a helical tomotherapy unit," Med. Phys. **32**(11), 3424–3430 (2005).
[13]J. Balog, G. Olivera, and J. Kapatoes, "Clinical helical tomotherapy commissioning dosimetry," Med. Phys. **30**(12), 3097–3106 (2003).
[14]R. T. Flynn, M. W. Kissick, M. P. Mehta, G. H. Olivera, R. Jeraj, and T. R. Mackie, "The impact of linac output variations on dose distributions in helical tomotherapy," Phys. Med. Biol. **53**(2), 417–430 (2008).
[15]P. Francois and A. Mazal, "Static and rotational output variation of a tomotherapy unit," Med. Phys. **36**(3), 816–820 (2009).
[16]P. R. Almond, P. J. Biggs, B. M. Coursey, W. F. Hanson, M. S. Huq, R. Nath, and D. W. Rogers, "AAPM's TG-51 protocol for clinical reference dosimetry of high-energy photon and electron beams," Med. Phys. **26**(9), 1847–1870 (1999).
[17]R. Alfonso, P. Andreo, R. Capote, M. Saiful Huq, W. Kilby, P. Kjäll, T. R. Mackie, H. Palmans, K. Rosser, J. Seuntjens, W. Ullrich, and S. Vatnitsky, "A new formalism for reference dosimetry of small and nonstandard fields," Med. Phys. **35**(11), 5179–5186 (2008).
[18]P. Andreo, D. T. Burns, K. Hohlfeld, M. S. Huq, T. Kanai, F. Laitano, V. G. Smyth, and S. Vynckier, IAEA Technical Report Series No. 398 (Vienna, 2000).
[19]S. D. Thomas, M. Mackenzie, D. W. Rogers, and B. G. Fallone, "A Monte Carlo derived TG-51 equivalent calibration for helical tomotherapy," Med. Phys. **32**(5), 1346–1353 (2005).
[20]M. McEwen, "Evaluation of the Exradin A19 ion chamber for reference dosimetry in megavoltage photon beams," Med. Phys. **34**(6), 2451 (2007).
[21]H. Keller, M. Glass, R. Hinderer, K. Ruchala, R. Jeraj, G. Olivera, and T. R. Mackie, "Monte Carlo study of a highly efficient gas ionization detector for megavoltage imaging and image-guided radiotherapy," Med. Phys. **29**(2), 165–175 (2002).
[22]P. F. Judy, S. Balter, D. Bassano, E. C. McCullough, J. T. Payne, and L. Rothenberg, "Phantoms for performance evaluation and quality assurance of CT scanners," AAPM Report No. 1 (American Association of Physicists in Medicine, Chicago, IL, 1977).
[23]K. J. Ruchala, G. H. Olivera, E. A. Schloesser, and T. R. Mackie, "Megavoltage CT on a tomotherapy system," Phys. Med. Biol. **44**(10), 2597–2621 (1999).
[24]A. P. Shah, K. M. Langen, K. J. Ruchala, A. Cox, P. A. Kupelian, and S. L. Meeks, "Patient dose from megavoltage computed tomography imaging," Int. J. Radiat. Oncol., Biol., Phys. **70**(5), 1579–1587 (2008).
[25]S. Boswell, W. Tome, R. Jeraj, H. Jaradat, and T. R. Mackie, "Automatic registration of megavoltage to kilovoltage CT images in helical tomotherapy: An evaluation of the setup verification process for the special case of a rigid head phantom," Med. Phys. **33**(11), 4395–4404 (2006).
[26]C. Woodford, S. Yartsev, and J. Van Dyk, "Optimization of megavoltage CT scan registration settings for brain cancer treatments on tomotherapy," Phys. Med. Biol. **52**(8), N185–N193 (2007).
[27]C. Woodford, S. Yartsev, and J. Van Dyk, "Optimization of megavoltage CT scan registration settings for thoracic cases on helical tomotherapy," Phys. Med. Biol. **52**(15), N345–N354 (2007).
[28]K. M. Langen, Y. Zhang, R. D. Andrews, M. E. Hurley, S. L. Meeks, D. O. Poole, T. R. Willoughby, and P. A. Kupelian, "Initial experience with megavoltage (MV) CT guidance for daily prostate alignments," Int. J. Radiat. Oncol., Biol., Phys. **62**(5), 1517–1524 (2005).
[29]E. T. Soisson, G. Sobering, D. Lucas, E. Chao, G. Olivera, and W. A. Tome, "Quality assurance of an image guided intracranial stereotactic positioning system," Technol. Cancer Res. Treat. **8**(1), 39–49 (2009).
[30]S. L. Meeks, J. F. Harmon, Jr., K. M. Langen, T. R. Willoughby, T. H. Wagner, and P. A. Kupelian, "Performance characterization of megavoltage computed tomography imaging on a helical tomotherapy unit," Med. Phys. **32**(8), 2673–2681 (2005).
[31]K. M. Langen, S. L. Meeks, D. O. Poole, T. H. Wagner, T. R. Willoughby, P. A. Kupelian, K. J. Ruchala, J. Haimerl, and G. H. Olivera, "The use of megavoltage CT (MVCT) images for dose recomputations," Phys. Med. Biol. **50**(18), 4259–4276 (2005).
[32]B. Fraass, K. Doppke, M. Hunt, G. Kutcher, G. Starkschall, R. Stern, and J. Van Dyke, "American Association of Physicists in Medicine Radiation Therapy Committee Task Group 53: Quality assurance for clinical radiotherapy treatment planning," Med. Phys. **25**(10), 1773–1829 (1998).
[33]G. H. Olivera, D. M. Shepard, K. Ruchala, J. S. Aldridge, J. M. Kapatoes, E. E. Fitchard, P. J. Reckwerdt, G. Fang, J. Balog, J. Zachman, and T. R. Mackie, in *The Modern Technology of Radiation Oncology*, edited by J. Van Dyk (Medical Physics, Madison, 1999), pp. 521–587.
[34]M. W. Kissick, J. Fenwick, J. A. James, R. Jeraj, J. M. Kapatoes, H. Keller, T. R. Mackie, G. Olivera, and E. T. Soisson, "The helical tomotherapy thread effect," Med. Phys. **32**(5), 1414–1423 (2005).
[35]D. C. Westerly, E. Soisson, Q. Chen, K. Woch, L. Schubert, G. Olivera, and T. R. Mackie, "Treatment planning to improve delivery accuracy and patient throughput in helical tomotherapy," Int. J. Radiat. Oncol., Biol., Phys. **74**(4), 1290–1297 (2009).
[36]T. R. Mackie, G. H. Olivera, J. M. Kapatoes, K. J. Ruchala, J. P. Balog, W. A. Tome, S. Hui, M. Kissick, C. Wu, R. Jeraj, P. J. Rockwerdt, P. Harari, M. Ritter, L. Forrest, J. S. Welsh, and M. P. Metha, "Helical Tomotherapy," in *Intensity-Modulates Radiation Therapy. The State of the Art*, AAPM Summer School Proceedings, edited by J. Palta and T. R. Mackie (Medical Physics, Madison, 2003), pp. 247–284.
[37]J. P. Gibbons, K. Smith, D. Cheek, and I. Rosen, "Independent calculation of dose from a helical TomoTherapy unit," J. Appl. Clin. Med. Phys. **10**(1), 103–119 (2009).
[38]G. A. Ezzell, J. W. Burmeister, N. Dogan, T. J. LoSasso, J. G. Mechalakos, D. Mihailidis, A. Molineu, J. R. Palta, C. R. Ramsey, B. J. Salter, J. Shi, P. Xia, N. J. Yue, and Y. Xiao, "IMRT commissioning: Multiple institution planning and dosimetry comparisons, a report from AAPM Task Group 119," Med. Phys. **36**(11), 5359–5373 (2009).
[39]J. Van Dyk, in *Treatment Planning in Radiation Oncology*, edited by F. M. Kahn and R. A. Potish (Williams and Wilkins, Baltimore, 1998), pp. 123–146.
[40]A. Van Esch, C. Clermont, M. Devillers, M. Iori, and D. P. Huyskens, "On-line quality assurance of rotational radiotherapy treatment delivery by means of a 2D ion chamber array and the Octavius phantom," Med. Phys. **34**(10), 3825–3837 (2007).
[41]M. Geurts, J. Gonzalez, and P. Serrano-Ojeda, "Longitudinal study using a diode phantom for helical tomotherapy IMRT QA," Med. Phys. **36**(11), 4977–4983 (2009).
[42]D. A. Low, W. B. Harms, S. Mutic, and J. A. Purdy, "A technique for the quantitative evaluation of dose distributions," Med. Phys. **25**(5), 656–661 (1998).
[43]R. Holly, S. Myrehaug, A. Kamran, R. Sankreacha, and G. Morton, "High-dose-rate prostate brachytherapy in a patient with bilateral hip prostheses planned using megavoltage computed tomography images acquired with a helical tomotherapy unit," Brachytherapy **8**(1), 70–73 (2009).
[44]S. Mutic and D. A. Low, "Whole-body dose from tomotherapy delivery," Int. J. Radiat. Oncol., Biol., Phys. **42**(1), 229–232 (1998).
[45]S. Baechler, F. O. Bochud, D. Verellen, and R. Moeckli, "Shielding requirements in helical tomotherapy," Phys. Med. Biol. **52**(16), 5057–5067 (2007).
[46]D. Robinson, J. W. Scrimger, G. C. Field, and B. G. Fallone, "Shielding considerations for tomotherapy," Med. Phys. **27**(10), 2380–2384 (2000).

[47]J. Balog, D. Lucas, C. DeSouza, and R. Crilly, "Helical tomotherapy radiation leakage and shielding considerations," Med. Phys. **32**(3), 710–719 (2005).
[48]C. Wu, F. Guo, and J. A. Purdy, "Helical tomotherapy shielding calculation for an existing LINAC treatment room: Sample calculation and cautions," Phys. Med. Biol. **51**(21), N389–N392 (2006).
[49]A. Zacarias, J. Balog, and M. Mills, "Radiation shielding design of a new tomotherapy facility," Health Phys. **91**(4), 289–295 (2006).
[50]P. H. McGinley, *Shielding Techniques for Radiation Oncology Facilities* (Medical Physics, Madison, 1998).